Gold Nanoparticles Based Electrochemical Biosensors

Thesis submitted for the Degree of

DOCTOR OF PHILOSOPHY

GAUTHAM KUMAR AHIRWAL

Department of Biochemistry
School of Life Sciences
University of Hyderabad
Hyderabad
2009

Gold Nanoparticles Based Electrochemical Biosensors

Thesis submitted for the Degree of

DOCTOR OF PHILOSOPHY

By

GAUTHAM KUMAR AHIRWAL

Department of Biochemistry
School of Life Sciences
University of Hyderabad
Hyderabad - 500 046
India

December 2009

Enrollment No: 04LBPH04

Dedicated to my Parents and Wife

UNIVERSITY OF HYDERABAD

Department of Biochemistry

School of Life Sciences

Certificate

This is to certify that this thesis entitled **"Gold Nanoparticles Based Electrochemical Biosensors"** submitted to the University of Hyderabad, Hyderabad by **Mr. Gautham Kumar Ahirwal** for the degree of Doctor of Philosophy, is based on the studies carried out by him under my supervision. I declare to the best of my knowledge that this work has not been submitted earlier for the award of degree or diploma from any other University or Institution.

Chanchal K Mitra
Supervisor

Head
Dept. of Biochemistry

Dean
School of Life Sciences

UNIVERSITY OF HYDERABAD

Department of Biochemistry

School of Life Sciences

Declaration

I hereby declare that the work presented in my thesis entitled **"Gold Nanoparticles Based Electrochemical Biosensors"** is entirely original and has been carried out by me in the Department of Biochemistry, University of Hyderabad, Hyderabad, under the supervision of **Prof. Chanchal K Mitra**. I further declare that this work has not been submitted earlier for the award of degree or diploma from any other University or Institution.

GAUTHAM KUMAR AHIRWAL
(Enrollment No. 04LBPH04)

Date:
Place: Hyderabad

Prof. Chanchal K Mitra
(Supervisor)

Acknowledgements

- *I express my sincere gratitude to our Prof. Chanchal K Mitra for his disciplined supervision, motivated guidance, valuable suggestions and constant encouragement throughout my work.*
- *I thank our Dean, Prof. A. S. Raghavendra for providing all the required facilities for the completion of my research work.*
- *I thank our Head Prof. K.V.A. Ramaiah and former Prof. M.Ramanadham for extending the facilities for the completion of my work.*
- *I thank Prof. Lo Gorton (University of Lund, Sweden) for his valuable suggestions and discussions.*
- *I thank Dr. Elena Kashuba (Karolinska Institute, Sweden) for allowing me to work with her group and try my hands on completely new work and also making the stay memorable.*
- *I thank the funding agencies (DBT, DST, CSIR, Indo-Swedish) for funding the lab.*
- *I thank CSIR for granting my fellowship.*
- *I thank all my lab mates, former lab mates, friends, Ramesh and well wishers for giving me all the support.*
- *I thank all the office and non-teaching staff for helping me during my work.*
- *I am very grateful to my parents, my wife, my brother and my sister for giving me all their love, support and encouragement.*
- *I am always thankful to GOD for giving me all the courage to overcome most of the difficulties in my life.*

Gautham Kumar Ahirwal

Table of contents

Chapter 1

Introduction

1.1 Introduction

Biosensor is an analytical device, which converts a biological response into an electrical signal (Figure 1). The term "biosensor" is often used to cover sensor devices used, in order to determine the concentration of substances and other parameters of biological interest even where they do not utilize a biological system directly. Biosensors represent a rapidly expanding field and the present time, it has much importance in major areas like health-care industry, food quality and environmental monitoring. Research and development in this field is wide and multidisciplinary, spanning biochemistry, bioreactor science, physical chemistry, electrochemistry, electronics and software engineering.

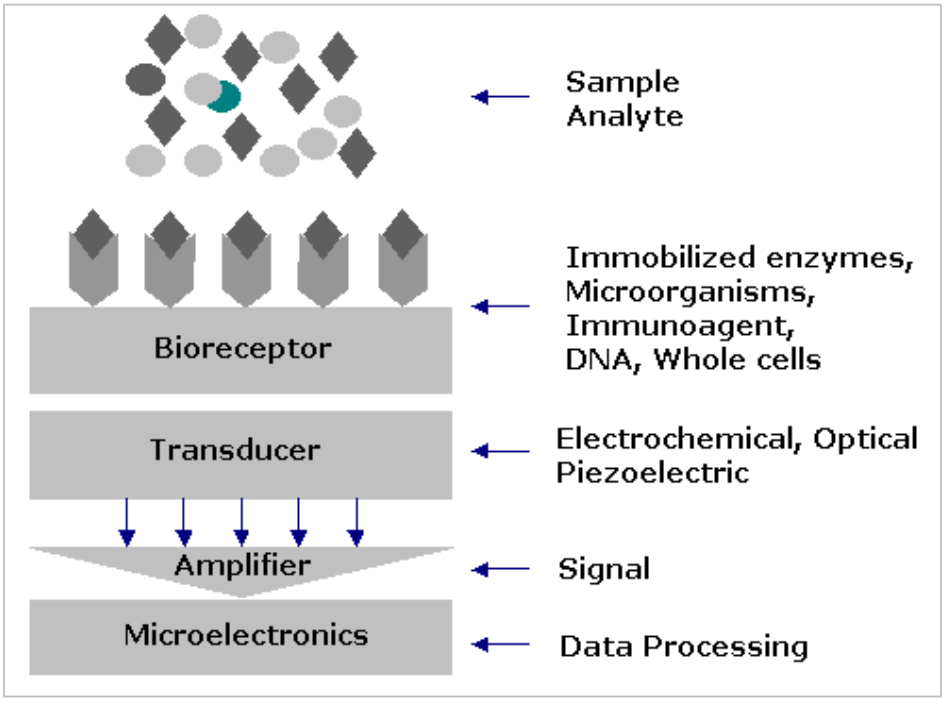

Figure.1. Schematic diagram showing the main components of a biosensor. The bioreceptor converts the substrate to product. The reaction is determined by the transducer and the signal is amplified, processed and displayed by microelectronics.

A successful biosensor must possess at least some of the following beneficial features:

- The biocatalyst must be highly specific for the purpose of the analyses, be stable under normal storage conditions and, show good stability over a large number of assays.
- The reaction should be as independent of such physical parameters as stirring, pH and temperature as is manageable.
- The response should be accurate, precise, reproducible and linear over the useful analytical range, without dilution or concentration.
- The response should be free from electrical noise.
- The biosensor should be small and biocompatible.
- The complete biosensor should be cheap, small, portable and capable of being used by semi-skilled operators.

- **Generation of an electronic signal:**

A transducer is used in a biosensor to convert a specific biological event (catalytic or binding) into an electronic response that can be displayed directly, which can be further processed by a microprocessor. In order to be successful, this transducer must also be amenable to the immobilization of the biological component with which it is in intimate contact. Many transducers have been used in the construction of biosensors and some of the most common ones are summarized in Table 1.

Table 1. Transducers commonly used in biosensors

Transducers	Examples
▪ **Electrochemical:**	
a) Amperometric	Clark oxygen electrode, mediated electrode systems.
b) Potentiometric	Redox electrodes, ion selective electrodes, field effect transistors.
c) Conductometric	Platinum or gold electrodes for the measurements of change in conductivity of the solution due to generation of ions.
▪ **Optical:**	Photodiodes, Waveguide systems, integrated optical sensors.
▪ **Acoustic:**	Piezoelectric crystals, surface acoustic wave devices
▪ **Calorimetric:**	Thermistor or thermopile.

1.1.1 Electrochemical transducers:

Electrochemical transducers have practical advantages such as operational simplicity, low cost of fabrication and real time detection.

1.1.1.1 Amperometric sensor:

Amperometry is based on the measurement of the current resulting from the electrochemical oxidation or reduction of an electroactive species (Scheller *et al*., 1982). It is usually performed by maintaining a constant potential at a Platinum (Pt), Gold (Au) or Carbon (C) based working electrode or on array of electrodes with respect to a reference electrode, which may also serve as the auxiliary electrode, if currents are low (from 10^{-9} to 10^{-6} A). The resulting current is directly correlated to the bulk concentration of the electroactive species or its production or consumption rate within the adjacent biocatalytic layer. As biocatalytic reaction rates are often chosen to be first

order dependent on the bulk analyte concentration, such steady-state currents are usually proportional to the bulk analyte concentration.

1.1.1.2 Potentiometric sensors:

Potentiometric measurements involve determination of the potential difference between either an indicator or a reference electrode, or two reference electrodes separated by a perm selective membrane, when there is no significant current flowing between them. The transducer may be an ion-selective electrode (ISE) which is an electrochemical sensor based on thin films or selective membranes as recognition elements. The most common potentiometric devices are pH electrodes; several other ion (F^-, I^-, CN^-, Na^+, K^+, Ca^{2+}, NH_4^+) or gas (CO_2, NH_3) selective electrodes are available (Scheller *et al*., 1989 and Kodo *et al*., 1980). The potential differences between these indicator and reference electrodes are proportional to the logarithm of the ion activity or gas fugacity (or concentration), as described by the Nernst-Donnan equation. This is only the case when (i) the membrane or layer selectivity is infinite or if there is a constant or low concentration of interfering ions; and (ii) potential differences at various phase boundaries are either negligible or constant, except at the membrane:sample-solution boundary. When a biocatalyst layer is placed adjacent to the potentiometric detector, one has to take into account of, as for any biocatalyst sensor: (1) transport of the substrate to be analysed to the biosensor surface; (2) analyte diffusion to the reacting layer; (3) analyte reaction in the presence of biocatalyst and (4) diffusion of reaction product towards both the detector and the bulk solution. The response of potentiometric biocatalytic sensors is, as for amperometric biosensors,

either steady-state or transient, but it is never an equilibrium response. The situation is more complex for enzyme-labelled immuno-sensors: although the Ab-Ag complex is expected to reach an equilibrium and reactions to be either reversible or irreversible, the labelled enzyme activity is measured under steady-state analyte consumption conditions.

1.1.1.3 Conductimetric sensors:

Many enzyme-catalyzed reactions are accompanied by conductivity changes, so that in principle, both enzymes and substrates can be assayed conductimetrically.

The earliest conductimetric measurements utilized the conversion of urea into ammonium and bicarbonate ions by the action of urease free in solution. Immobilization of the enzymes close to a platinum electrode enabled the development of a true biosensor. Microfabrication techniques have been used to produce interdigited microelectrodes in order to increase sensitivity. Such systems have enabled urea solutions at concentration as low as $1mmol^{-1}$ to give measurable conductance changes in less than two minutes. It is important to select the buffer used in conductance assays, since both the basic and acidic forms of the buffer directly participate in the overall conductance change during a reaction.

Another interesting conductimetric biosensor format is to incorporate a dual sensor configuration, one sensor with enzyme and one without as a control reference. This increases both sensitivity and selectivity.

1.1.2 Optical sensors:

Optical transducers detect the changes in optical properties like absorption, fluorescence, chemiluminescence, and refraction. Most of these transducers comprise of a light source, optical fiber and an appropriate optical detector. We can represent in the following way.

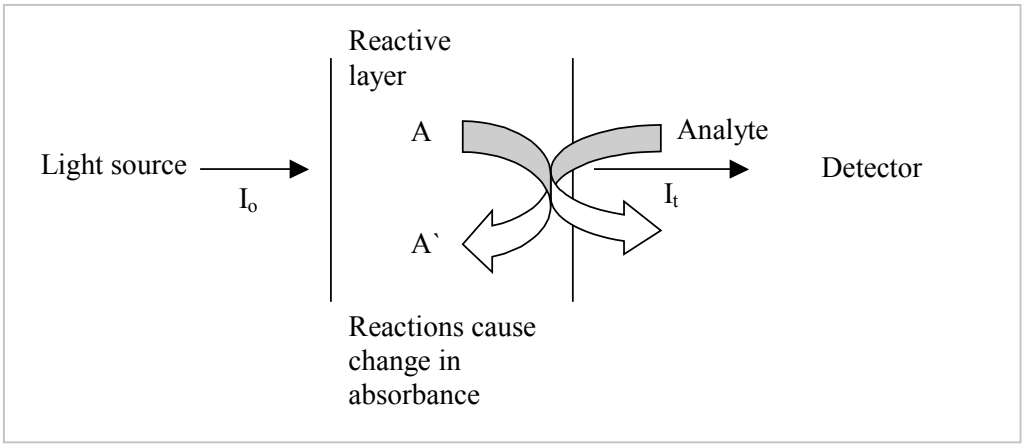

Optical sensors have several advantages of which the absence of their susceptibility to disturbances by electric field is the main advantage.

1.1.3 Acoustic sensors:

The principle of this sensor is that the frequency of vibration of an oscillating crystal is decreased by the adsorption of a foreign material on its surface. The crystal is sensitized by covering it with the biological element that react with the analyte to be determined (Bastains, 1988). Added to the very minute changes in the frequency of vibration upon the analyte binding to the sensing element, needs a highly sensitive device to recognize the signal and the difficulty for the adaptation of this technique to aqueous systems.

1.1.4 Calorimetric sensors:

All chemical processes exhibit enthalpy change. This can be measured by sensitive thermistors and can be related to the amount of reaction. The main advantage of the thermal transducers is its broad universal applicability. Because the enthalpy changes observed are very small for the biological reactions, highly sensitive thermistors have to be used.

1.1.5 Biological sensing element:

The biological response of the biosensor is determined by the biocatalytic membrane, which accomplishes the conversion of reactant to product. Immobilised enzymes possess a number of advantageous features, which makes them particularly applicable for use in such systems. They may be re-used, which ensures that the same catalytic activity is present for a series of analyses. This is an important factor in securing reproducible results and avoids the pitfalls associated with the replicate pipetting of free enzyme, otherwise necessary in analytical protocols. Many enzymes are intrinsically stabilised by the immobilisation process, but even where this does not occur there is usually considerable apparent stabilisation. It is normal to use an excess of the enzyme within the immobilised sensor system. Even where there is some inactivation of the immobilised enzyme over a period of time, this inactivation is usually steady and predictable.

The techniques for immobilizing biological sensing elements comprises of physical and chemical methods as well as combination of both.

1.1.5.1 Adsorption:

This method for the immobilization of a biomolecule is based on the physical adsorption of biomolecule on the surface. Hence, the method causes little or no conformational change of the biomolecule or destruction of its active center. If a suitable carrier is found, this method can be both simple and cheap. However, it has the disadvantage that the adsorbed biomolecule may leak from the carrier during use due to a weak binding force between the biomolecule and the carrier (Nelson *et al*., 1960). A major advantage of adsorption as a general method of immobilizing enzymes is that usually no reagents and only a minimum of activation steps are required. Adsorption tends to be less disruptive to the enzymatic protein than chemical means of attachment because the binding is mainly by hydrogen bonds, multiple salt linkages, and Vander Waal's forces (Carr *et al*., 1980). In this respect, the method bears the greatest similarity to the situation found in natural biological membranes and has been used to model such systems. Because of the weak bonds involved, desorption of the protein resulting from changes in temperature, pH, ionic strength or even the mere presence of substrate, is often observed. Another disadvantage is non-specific, further adsorption of other proteins or other substances as the immobilized biomolecule is used. This may alter the properties of the immobilized biomolecule or, if the substance adsorbed is a substrate for the enzyme, the rate will probably decrease depending on the surface mobility of biomolecule and substrate.

1.1.5.2 Gel entrapment:

In this method the biomolecules are entrapped in a matrix formed by organic polymers. Entrapment in polymeric gels prevent the biomolecules from diffusing and on the other hand the small substrate and effector molecules can easily permeate through them. Except for the use of strong chemicals during the formation of gels, which may impair the biological function. The commonly used entrapment media are polyacrylamide, gelatin and calcium alginate.

1.1.5.3 Covalent coupling:

The immobilization of biomolecules by covalent coupling usually leads to very stable preparation with extended active life when compared to the other immobilization methods, namely, physical adsorption and ionic binding.

The covalent binging method is based on the covalent attachment of biomolecules to matrices. This method has been the most wide spread and one of the most thoroughly investigated approaches for immobilization. Covalent binding is strong; there is no loss of biomolecule into the solution, even in the presence of strong ionic solutions. The immobilization of biomolecules by covalent attachment to a matrix involves the functional groups of the enzymes that are neither essential for its biological action nor for its function.

The three main factors that should be taken into account for the covalent immobilization of the biomolecule by a specific method are: (1) the functional group of biomolecule suitable for coupling under mild conditions, (2) the

coupling reaction between the biomolecule and the matrix surface, (3) the fuctionalized matrix suitable for biomolecule.

The major classes of coupling reactions used for the immobilization of biomolecules are:

- Diazotization
- Amide (peptide) bond formation
- Alkylation and arylation
- Schiff's base formation
- Ugi reaction
- Amidination reactions
- Thiol-disulfide interchange reactions
- γ-irradiation induced coupling

1.1.5.4 Crosslinking:

The biomolecules may be cross-linked with each other or to a matrix. The biomacromolecules can also be adsorbed to a water insoluble carrier or entrapped in a gel and then cross-linked. The advantages of crosslinking are its simple procedure and strong chemical binding of the biomolecules. The main drawback is the possibility of activity loss due to chemical alterations of the essential catalytic sites. The most commonly used cross-linker is glutaraldehyde.

1.1.6 Types of biosensors:

Based on the degree of intimacy between the biological substances and the transducers, biosensors are categorized as first, second and third generation instruments. First generation biosensors where the normal product of the reaction diffuses to the transducer and causes the electrical response, second generation biosensors which involve specific 'mediators' between the reaction and the transducer in order to generate improved response (Cass *et al*., 1984), and third generation biosensors where the reaction itself causes the response and no product or mediator diffusion is directly involved (Ghindilis *et al*., 1997).

1.1.7 Electrochemistry:

Electrochemistry is the study of reactions in which charged particles (ions or electrons) cross the interface between two phases of matter, typically a metallic phase (electrode) and a conductive solution or electrolyte.

1.1.7.1 The electrochemical cell:

A simple electrochemical cell consists of two electrodes and an electrolyte. An electrode is the interface at which dissolved substrates may pick up or lose electron(s). An electrolyte is needed in order to provide electrical conductivity between the two electrodes. In a cell used for electroanalytical measurements e.g. cyclic voltammetry, anonic stripping voltammetry, etc there are always three electrodes due to the difficulties arising because of the concurrent measurement of current and potential (Figure 2).

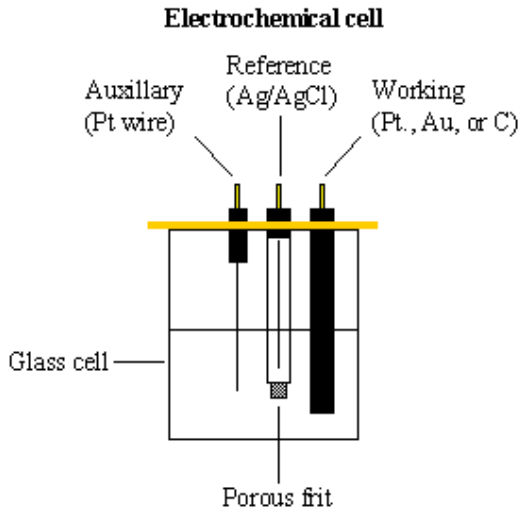

Figure. 2. A Typical three electrode setup consisting of a working electrode, a reference electrode and a auxiliary or counter electrode

- **Working electrode:** The first of the three electrodes is the indicating electrode also known as the test or working electrode. The working electrode is the electrode in an electrochemical system on which the reaction of interest is occurring, where the potential is controlled and the current is measured. The working electrode is often used in conjunction with an auxiliary electrode, and a reference electrode in a three-electrode system. Depending on whether the reaction on the electrode is a reduction or an oxidation, the working electrode can be referred to as either cathodic or anodic. Common working electrodes can consist of inert metals (such as gold, silver or platinum), to inert carbon (such as glassy carbon or pyrolytic carbon), mercury drop and film electrodes.

- **Reference electrode:** The second functional electrode is the reference electrode. This is the electrode whose potential is constant enough that

it can be taken as the reference standard, against which the potentials of the other electrodes present in the cell can be measured (Ives *et al*., 1961). Commonly used reference electrodes are the silver-silver chloride electrode (Ag/AgCl/4M KCl, e=0.222 V) or the calomel electrode (Hg/HgCl/KCl).

- **Counter electrode:** The final functional electrode is the counter or auxiliary electrode, which serves as a source or sink for electrons so that current can be passed from the external circuit through the cell. In general, neither its true potential nor the current is ever measured or known.

1.1.7.2 Voltammetric techniques:

Voltammetry is a category of electroanalytical methods used in analytical chemistry and various industrial processes. In voltammetry, information about an analyte is obtained by measuring the current as the potential is varied. Voltammetry experiments investigate the half cell reactivity of an analyte. Most experiments control the potential (Volts) of an electrode in contact with the analyte while measuring the resulting current (Amperes).

To conduct such an experiment it requires at least two electrodes. The working electrode, which makes contact with the analyte must apply the desired potential in a controlled way and facilitate the transfer of electrons to and from the analyte. A second electrode acts as the other half of the cell. This second electrode must have a known potential which is used to gauge the potential of

the working electrode, furthermore it must balance the electrons added or removed by the working electrode. While this is a viable setup, it has a number of shortcomings. Most significantly, it is extremely difficult for an electrode to maintain a constant potential while passing current to counter redox events at the working electrode.

To solve this problem, the role of supplying electrons and referencing potential has been divided between two separate electrodes. The reference electrode is a half-cell with a known reduction potential. Its only role is to act as reference in measuring and controlling the working electrodes potential and at no point does it pass any current. The auxiliary electrode passes all the current needed to balance the current observed at the working electrode. To achieve this current, the auxiliary electrode will often swing to extreme potentials at the edges of the solvent window, where it oxidizes or reduces the solvent or supporting electrolyte. These electrodes, the working, reference, and auxiliary make up the modern three-electrode system.

Types of Voltammetry:

(i) Linear sweep voltammetry:

It is a voltammetric method where the current at a working electrode is measured while the potential between the working electrode and a reference electrode is swept linearly in time (Figure 3). Oxidation or reduction of species is registered as a peak or trough in the current signal at the potential at which the species begins to be oxidized or reduced.

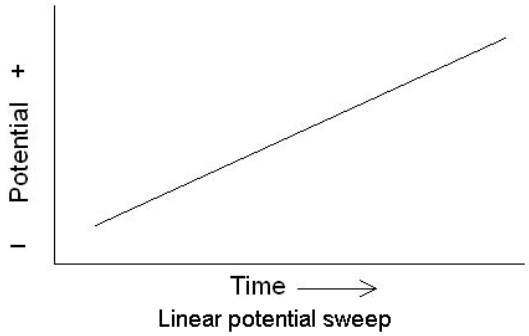

Figure.3. Typical waveform of Linear potential sweep.

(ii) Staircase voltammetry:

It is a derivative of linear sweep voltammetry. In linear sweep voltammetry the current at a working electrode is measured while the potential between the working electrode and a reference electrode is swept linearly in time. Oxidation or reduction of species is registered as a peak or trough in the current signal at the potential at which the species begins to be oxidized or reduced. In staircase voltammetry the potential sweep is a series of stair steps. The current is measured at the end of each potential change, right before the next, so that the contribution to the current signal from the capacitive charging current is minimized (Figure 4).

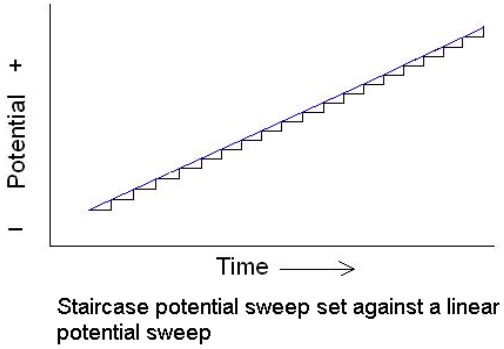

Figure.4. Typical Staircase voltammetry waveform.

(iii)Squarewave voltammetry:

This technique is a further improvement of staircase voltammetry, which is itself a derivative of linear sweep voltammetry. In linear sweep voltammetry, the current at a working electrode is measured while the potential between the working electrode and a reference electrode is swept linearly in time. Oxidation or reduction of species is registered as a peak or trough in the current signal at the potential at which the species begins to be oxidized or reduced. In staircase voltammetry the potential sweep is a series of stair steps. The current is measured at the end of each potential change, right before the next, so that the contribution to the current signal from the capacitive charging current is minimized. In squarewave voltammetry, a squarewave is superimposed on to the potential staircase sweep. The current is measured at the end of each half-wave, just prior to the potential change. The differential current is then plotted as a function of potential, and the reduction or oxidation of species is measured as a peak or trough (Figure 5).

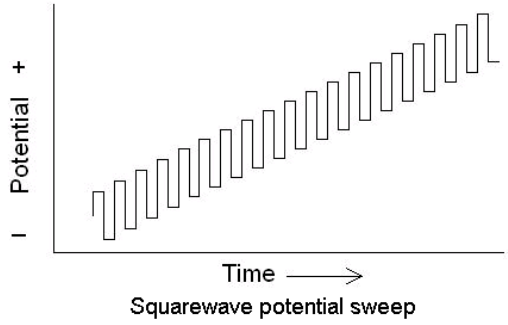

Figure.5. Typical Square wave voltammetry waveform.

(iv) Cyclic voltammetry (CV):

CV one of the more commonly used electroanalytical techniques, is an excellent methods development tool, but is not usually a good technique for quantitative analysis. Its main advantage in electroanalysis is its ability to characterize an electrochemical system.

A single CV experiment only hints at the events that constitute the electrochemical reaction at the electrode. However, multiple CV experiments can be used for a variety of applications, including:

• The determination of Nernstian (reversible) or non-Nernstian (irreversible) behavior of a redox couple

• The number of electrons transferred in an oxidation or reduction

• Formal potentials

• Rate constants

• Formation constants

• Reaction mechanisms

• Diffusion coefficients

In a CV experiment, the potentiostat applies a potential ramp to the working electrode to gradually change the potential and then reverses the scan, returning to the initial potential (see the triangular waveform in Figure 6).

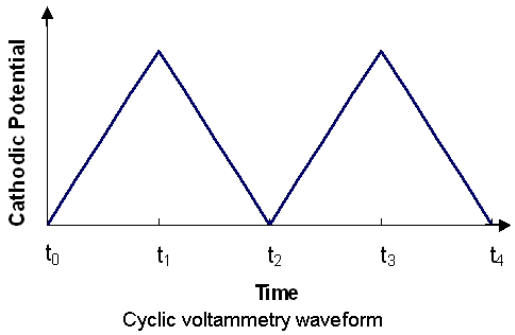

Figure.6. A typical Cyclicoltammetry waveform.

During the potential sweep, the potentiostat measures the current resulting from the applied potential. These values are then used to plot the CV graph of the current versus the applied potential. You can run single-cycle or multi-cycle CV experiments. The repetition of the potential waveform allows the system to come to a steady-state or allows the buildup of reaction products at the electrode surface. Figure 7 is a typical CV plot, which shows the four important pieces of information obtained from a CV experiment—the cathodic peak height (I_{pc}), the anodic peak height (I_{pa}), the cathodic peak potential (E_{pc}) and the anodic peak potential (E_{pa}). Note that Figure 7 uses the American convention for plotting electrochemical data—that is, negative potential to the right and the positive potential to the left of the plot. The cathodic (reductive) current (upward) and the anodic current are represented downwards.

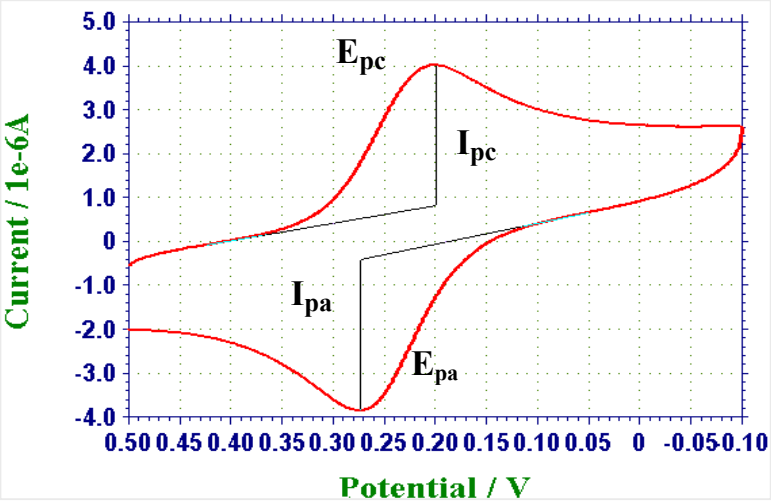

Figure.7. Typical plot of a cyclic voltammetry or cyclic voltammogram.

- **Single CVs:**

A single CV is useful for determining whether or not a species is electroactive. A peak current response within a given potential range indicates whether a material has been involved in a reaction or not. However, from a single CV plot, we can draw only limited conclusions about the reversibility of a redox couple. One criterion for reversibility is that the I_{pc} should be equal to I_{pa}, so that it may seem, that if a single CV shows I_{pc} equal to I_{pa}, the system is reversible. However, if the scan rate is increased the I_{pc} may no longer be equal to I_{pa} and the system would appear irreversible. The same can be true of other variables in the experiment. A change of concentration or electrolyte could also affect the results of the experiment. Thus a single CV is only useful to define reversibility for a very specific set of experimental conditions.

A single CV is also useful in determining the number of electrons transferred in a reaction. If we assume the reaction is reversible (i.e., it follows the Nernst equation) wecan calculate the number of electrons transferred during the oxidation/reduction. The current maximum for each peak should be 28.5 mV from the formal potential; the potential difference between E_{pa} and E_{pc} should be 59 mV (Nicholson *et al*., 1964). These values are good for a one-electron transfer. In general the peak separation is expressed as given below.

$$\Delta E = \frac{59\ mV}{n}$$

Where n is the number of electrons tansferred.

- **Muliple CVs:**

This allows us to see chemical changes with time or allows a system to reach equilibrium before the measurements are made. In fact, the diagnostic information explained above for a single CV is more appropriately used after two or three cycles of the CV are run. Multiple CV experiments also allow us to observe reaction products formed at the surface of an electrode that may not be stable.

In a typical CV study, we run a series of experiments in which we selectively vary the potential scan rate, the experiment temperature, the species concentration or the ionic strength of the supporting electrolyte. We can vary the scan rate in a series of experiments to determine the diffusion coefficient of a species. In this approach, we

plot the I_{pc} versus the square root of the scan rate (Honey *et al*., 1998). For a reversible system, the peak height will increase linearly with the square root of the

$$i_p = 269n^{3/2}AD^{1/2}v^{1/2}C^b$$

Where
i_p = peak height (amp)
n = number of electrons
A = area (cm^2)
D = deffusion coefficient (cm^2 /sec)
v= scan rate (V/sec)
C^b = bulk concentration of solution (M)

scan rate. The slope of the resulting line will be proportional to the diffusion coefficient, as shown in the Randles-Sevcik equation

(v) Pulse Methods:

In order to increase the speed and sensitivity, many forms of potential modulations (other than just a simple staircase ramp) have been tried, over the years. Two of these pulse techniques are shown in the Figure 8.

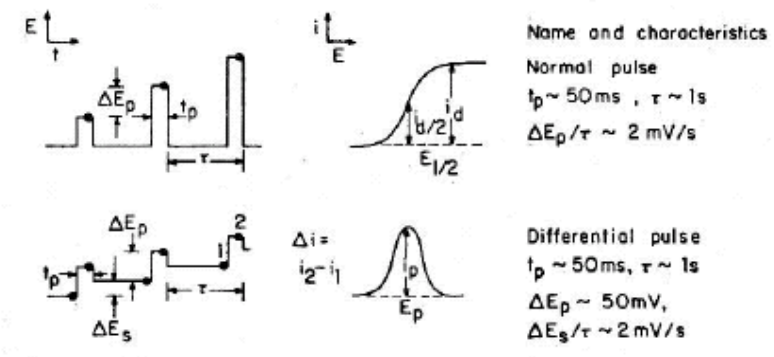

Figure.8. Potential waveforms and their respective current response for the Normal pulse and Differential pulse voltammetry.

- **Normal Pulse Voltammetry (NPV):**

This technique uses a series of potential pulses of increasing amplitude. The current measurement is made near the end of each pulse, which allows time for the charging current to decay. It is usually carried out in an unstirred solution at either DME (called normal pulse polarography) or solid electrodes. The potential is pulsed from an initial potential *Ei*. The duration of the pulse, t, is usually 1 to 100 msec and the interval between pulses typically is 0.1 to 5 sec. The resulting voltammogram displays the sampled current on the vertical axis and the potential to which the pulse is stepped on the horizontal axis.

- **Differential Pulse Voltammetry (DPV):**

This technique is comparable to normal pulse voltammetry in that the potential is also scanned with a series of pulses. However, it differs from NPV because each potential pulse is fixed, of small amplitude (10 to 100 mV), and is superimposed on to a slowly changing base potential. Current is measured at two points for each pulse, the first point (1) just before the application of the pulse and the second (2) at the end of the pulse. These sampling points are selected to allow for the decay of the nonfaradaic (charging) current. The difference between current measurements at these points for each pulse is determined and plotted against the base potential.

1.1.7.3 Electrochemical Impedance Spectroscopy (EIS):

Electrochemical impedance spectroscopy is a power tool for examining many chemical and physical processes in solutions as well as solids. For solution phase electrochemistry, a complex sequence of coupled processes such as, electron transfer, mass transport and chemical reaction can all control or influence the output from an electrochemical measurement.

EIS is an effective method to monitor the changes of the surface modified electrodes allowing the understanding of the chemical transformation and processes associated with the conductive electrode (Bard and Faulkner, 1980). The impedance spectra include a semicircle portion and a linear portion, the semicircle portion at higher frequencies corresponds to the electron transfer limited process and the linear part at lower frequencies corresponds to the diffusion process. The semicircle corresponds to the electron transfer resistance.

In impedance measurements, a sinusoidal potential (E_{ac}) is superimposed on a dc potential (E_{dc}). E_{ac} can be described by the equation 1,

$$E_{ac} = E_0 \sin \omega t \qquad \text{(Equation 1)}$$

Where E_0 is the amplitude (V), t is the time (s), and ω is the radial frequency (rad s^{-1}). The response is the current I given by equation 2,

$$I = I_0 \sin(\omega t + \phi) \qquad \text{(Equation 2)}$$

Where φ is the phase angle between perturbation and response. The proportionality factor between E and I is the impedance Z.

The current through a resistance R is given by the equation 3,

$$I = \frac{E_0}{R}\sin\omega t \qquad \text{(Equation 3)}$$

Kinds of resistances that are found in the electrochemical cells are:

- Solution resistance (R_s), which depends on the ionic strength of the solution and the distances between the working, auxiliary and reference electrode
- Polarization resistance (R_p), which arises from the application of a potential other than its equilibrium potential to the electrode
- Charge transfer resistance (R_{ct}), which is due to the electron transfer of a redox probe to the electrode

The current through a capacitance C is given by the equation 4,

$$I = C\frac{dE}{dt}\cos\omega t \qquad \text{(Equation 4)}$$

which implies a phase angle ($\varphi = \pi/2$) between the potential and the current. The capacitance of the working electrode is built up from the capacitances of the layers on the electrode and the electrical double layer. Because the latter is relatively large, its contribution to the total capacitance is negligible. In an immunosensor, therefore, the total capacitance (C_{dl}) is determined by that of the immobilized antibodies (C_{Ab}). When the antigen binds, a hydrophobic layer is formed in contact with the antibodies, with a capacitance C_{Ag}, and C_{dl} decreases according to the equation 5.

$$\frac{1}{C_{dl}} = \frac{1}{C_{Ab}} + \frac{1}{C_{Ag}} \qquad \text{(Equation 5)}$$

Data obtained by scanning ω automatically can be plotted in a Nyquist plot. Here, Z is a vector, which can be separated in an in-phase (Z') and out-of-phase (Z'') component. These systems are often be described by the Randles' equivalent circuit (Figure 9a). From Figure 9b, R_s and R_{ct} can be calculated from the intercept with the Z'-axis, and C_{dl} from ω at Z''_{max}. Z_w is the Warburg impedance, which indicates mass-transfer through the boundary layer on the electrode. At low frequencies, diffusion can rule the process (mass-transfer control). In this case the impedance Z is the Warburg impedance, with $\varphi = \pi/4$ (Bard and Faulkner, 1980, Brett and Brett, 1993) At high frequencies, the process is kinetically controlled and the influence of Z_w is negligible, which leads to a semi-circle (Figure 9b). Electrodes do not behave ideally, e.g., because of the roughness of the surface and the complicated structure of an immobilized antibody layer. A constant-phase element (Q) is used to describe these systems more appropriately. Its impedance (Z_Q) is described by $Y0\ (j\ \omega)^{-n}$, where Y_0 is a proportionality constant, $j = \sqrt{-1}$, and n is an exponent ($-1 \leq n \leq 1$). Although the exact physical basis of Q has to be elucidated, Q can be used for fitting the data in a very flexible way. If $n = 1$ the element $Y_0 = 1/C$ and if $n = 0$ $Y_0 = R$. Usually n has values between 0.7 and 0.9 in the case of solid electrodes (Zoltowski, 1998, Brett and Brett, 1993)

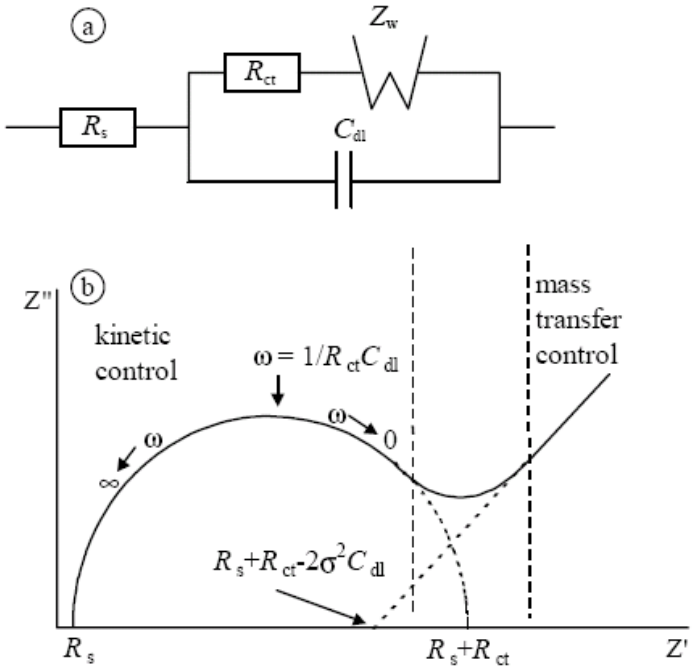

Figure. 9. (a) Randles' equivalent circuit , (b) Nyquist plot arising from a Randles'circuit.

The capacitance can be calculated using cyclic voltammetry (CV) or linear sweep voltammetry (LSV) by dividing the charging current in the potential scans by the scan rate (Chidsey *et al*., 1990 and Cheng *et al*., 1995). From the kinetics of the charge transfer of a redox probe, the amount of shielding of the electrode can be derived.

Current Approach:

So, with this knowledge of biosensors and electrochemical techniques, I carried out my reach work in order to study the electrochemistry of gold nanoparticles-biomolecule conjugate. The biomolecule (enzyme and antibody) was linked to the capped gold nanoparticles using carbodiimide crosslinking agent and was used for the electrochemical studies. In this regard, I have divided my research work into three sections and put forward some of the objectives, which are as follows:

1. ***Synthesis of Gold Nanoparticles***
2. ***Direct Electrochemistry of Horseradish Peroxidase-Gold Nanoparticles Conjugate***
3. ***Gold Nanoparticles Based Sandwich Electrochemical Immunosensor***

The following chapters give a detailed description (including introduction, methodology, results and discussions and conclusions) of each of the work done.

1.2 References

- Bastians, G. J. (1988). Chemical sensors, (Eds. J. E. Edmonds), Blakie, Glasglow, UK.
- Bard, A. J.; Faulkner, L. R. (1980). Electrochemical methods Fundamentals and Applications, John Wiley & Sons Ltd: New York, USA.
- Brett, C. M.; Oliveira Brett, A. M. (1993). Electrochemistry, principles, methods and applications, Oxford University Press, Inc.: New York, USA.
- Carr, P. W., Bowers, L. D. (1980). Immobilised enzymes in analytical and clinical chemistry, Wiley, New York.
- Cass, A. E. D., Davis, G. (1984). Ferrocene-mediated enzyme electrode for amperometric determination of glucose, *Anal. Chem*., 56, 667-671.
- Chidsey, C. E. D.; Loiacono, D. N. (1990). Chemical functionality in self-assembled monolayers: Structural and electrochemical properties, *Langmuir,* 6, 682-691.
- Cheng, Q.; Brajter-Toth, A. (1995). Permselectivity and high sensitivity at ultrathin monolayers. Effect of film hydrophobicity, *Anal. Chem*., 67, 2767-2775.

- Ghindilis, A L., Atanasov, P., Wilkins, E. (1997). Enzyme-catalyzed direct electron transfer: Fundamentals and analytical applications, *Electroanalysis*, 9, 661-664.
- Honey, M. J. C., Rechnitz, G. A. (1998). Voltammetry of Adsorbed Molecules. Part 1: Reversible Redox Systems, *Electroanalysis*, 10, 285.
- Ives, D. J, G., Ivans, E. J. (1961). General and theoritcal introduction: Reference electrodes, Academic press, New York 1-70.
- Kobos, R. K. (1980). Ion selective electrodes in analytical chemistry, (Eds. H. Fresier), Vol 2, Plenum-New York.
- Nelson, J. M., Griffin, E. J. (1916). Adsorption of invertase, *J. Am. Chem Soc*., 38, 1109-1115.
- Nicholson, R. S., Shain, I. (1964). Theory of Stationary Electrode Polarography. Single Scan and Cyclic Methods Applied to Reversible, Irreversible, and Kinetic Systems, *Anal. Chem*., 36, 706.
- Samuel, P. K. (1998). Voltammetric techniques in "Handbook of instrumental techniques for analytical chemistry", 709-725. http://www.prenhall.com/settle/chapters/ch37.pdf
- Scheller, F., Schubert, F. (1982). Fundamental of biosensors in "Biosensors", Elsevier Science Publishers, New York, 24-33.
- Scheller, F., Scbert, F. (1989). Research and development of biosensors. A review, *Analyst*, 114, 653-662.

- Zoltowski, P. (1998). On the electrical capacitance of interfaces exhibiting constant phase element behaviour, *J. Electroanal. Chem*., 443, 149-154.

Chapter 2

Synthesis of Gold Nanoparticles

2.1 Introduction

Gold (Au) as a precious material was first extracted in the 5th millennium BCE (Daniel *et al*., 2004). The soluble gold, which we now call colloid gold, was developed around the 4th or 5th century BCE (Daniel *et al*., 2004). Even though several scientists studied the formation and synthesis of colloidal Au, such as using phosphorous to reduce chloroaurate ($AuCl_4^-$) (Warner *et al*., 2003), colloid gold did not gain wide attention or became a subject of broad interest in the scientific community until very recently, especially in the last decade. The recent interest in such tiny Au particles partially arises from the commercial and industrial needs for new, advanced materials. These particles are nanometer size materials with unique optic, electronic, and magnetic properties. Biomolecules, also in the nanometer size range, possess functionalities that enable recognition and self-assembly. The integration of nanoparticles and biological molecules is very attractive and has gained tremendous attention from academics and industry, because such a combination could create new materials for electronics and optics, and lead to new applications in the broad areas of genomics, proteomics, and biomedical and bioanalytical devices (Kreibig *et al*., 1995, Motesharei *et al*., 1994, Mirkin *et al*., 2000, Sastry *et al*., 1998, Fitzmaurice *et al*., 1999, Mann *et al*., 2000, Storhoff *et al*., 1998, Hu *et al*., 2003, Kumar *et al*., 2008, Parak *et al*., 2003, Tkachenko *et al*., 2003). To be integrated with biological molecules or be used in biological systems, Au nanoparticles (AuNPs) have to be soluble in aqueous solution and have to be strongly dependant upon their physiochemical

characteristics and interaction with various surface moieties (protection of gold colloid). Gold nanoparticles stand apart from other nanoparticles and quantum dots because of their biocompatibility. The presence of gold nanoparticles (AuNP) provides more freedom in the orientation of the immobilized protein molecule thus permitting proteins to orient for directed interaction. Gold nanoparticles have been used for coupling to proteins (Burt *et al*., 2004), DNA (Cai *et al*., 2001, Amirkin *et al*., 1996, Castaneda *et al*., 2007) and RNA in various applications like immunoassays (Dequaire *et al*., 2000 and Kumar *et al*., 2008), detection of analytes (Tang *et al*., 2007, Authier *et al*., 2001, Li *et al*., 2006, Dua *et al*., 2005), and toxic compounds (Hua *et al*., 2003), for nuclear targeting (Tkachenko *et al*., 2003), as carrier agents (Wang *et al*., 2007), and has also been coupled to enzymes for biosensors (Xian *et al*., 2000, Liu *et al*., 2003, Ju *et al*., 2002, You *et al*., 2005, Gole *et al*., 2001).

Generally gold nanoparticles are synthesized by the reduction of an aurate salt with reducing agents, such as sodium borohydride ($NaBH_4$), thiocyanate, phosphorus, citrate and ascorbate. The synthesized nanoparticles are of nanometer size, with colors varying from yellow-orange to red-purple to blue-green. The color in terms of wavelength ranges from 510 to 550 nm.

2.1.1 Formation of AuNPs:

Gold nanoparticles can be produced by the reduction of gold ions. In the solution of tetrachloroauric acid ($HAuCl_4$), addition of reducing agents

nucleates the gold particles. Gold ions adsorb electrons from the reducing agents and become atoms as described in the chemical reaction below.

$$HAuCl_4 + 3e^- = Au^0 + H^+ + 4Cl^-$$

where the core of Au^0 nucleates when reducing agents provide e^-.

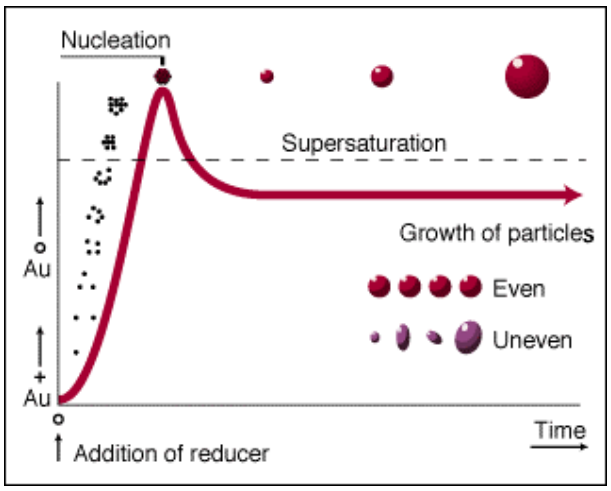

Figure 1. Nucleation of gold nanoparticles.

Several atoms aggregate to form a nucleation centre in particular nanostructure. A minimum of 11 atoms forms central icosahedral gold cores as shown in Figure 1, and the nanoparticles size and shape depends on the process environment. The particles become gold colloid due to the electronic shield on the surface. A solid double interfacial ionic layer surrounds colloidal gold particle. The core of pure gold is shielded by a layer of adsorbed $AuCl_2^-$ or Cl^- ions. Then, the hydrogen ions (H^+) in the solution are attracted by those negative charges and form the electrical double layers. The shield layer does the function of preventing nanoparticles from aggregation by the electrostatic repulsion. The electrical double layer is also involved in various adsorption, modification and other physical properties of the colloid.

2.1.2 Functionalization of gold nanoparticles:

Nanoparticles have to be surface modified to make them stable and compatible for preparation of bioconjugate. Some functional groups, such as cyano+ (-CN), thiol (-SH) and amino ($-NH_2$) groups are known to have high affinity for gold and the molecules having such functional groups can be used as capping agents for gold nanoparticles. Different methods have been developed till now for the synthesis and protection of the gold nanoparticles apart from the classical methods (Fren *et al*., 1973, Brust *et al*., 1995, Brust *et al*., 1994), using tryptophan (Selvakannan *et al*., 2004), amines (Subramaniam *et al*. 2005, Aslam *et al*., 2004) cinnamic acid (Wang *et al*., 2006), polypeptides stabilized (Yonezawa *et al*., 2006, Porta *et al*., 2007), ethylene glycol protected (Zheng *et al*., 2003), glutathione (Basu *et al*., 2007), lipoic acid-Poly (γ-benzyl-L-glutamate) (Yonezawa *et al*., 2006).

2.1.3 Choice of the AuNPs size:

For example, particles of 1 nm diameter would be virtually impossible to see, no matter how many had accumulated, because 1 nm particles do not have the bright red color of the larger sizes. It is not until particles reach 20 nm size at a worthwhile signal can be seen. Steric hindrance becomes a problem as the particles increase in size (Figure 2). For example, if an IgG molecule (160,000 daltons) is just 8 nm in length, only approximately 4 nm of this will extend from the surface of a gold particle. Particles of 100 nm will tend to dwarf the small surface molecules and make it difficult for them to interact with specific proteins. In other words, the larger the particle size, the

fewer of them will be present in a given volume of solution (starting with the same molar concentration of gold colloid).

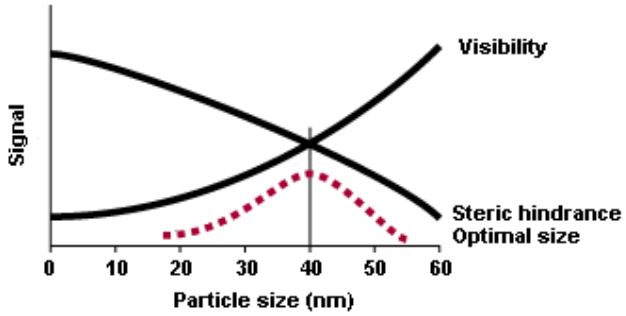

Figure 2. Choice of gold particle size for optimized signal.

This trade-off between required visibility and steric hindrance dictates that, for most immunoassay applications, the optimum particle size is 40 nm. In some cases where steric hindrance is a greater problem (e.g., for smaller antigens), particles of 20 nm are preferred. In general, particles of size 20-40 nm are commonly used in modern applications

2.2 Materials and methods

2.2.1 Materials:

$AuCl_4 4H_2O$ (Au% > 49%) and all other chemicals were of the analytical grade and were used without further purification. All solutions were prepared using double distilled water.

2.2.2 Instrumentation:

The absorption spectrum of the samples was recorded with an UV-1601 spectrophotometer (Shimadzu). FTIR spectra of the samples were collected on a Jasco type 5300 FTIR spectrometer using KBr mulls.

2.2.3 Methodology:

2.2.3.1 Synthesis of sodium borohydride reduced gold nanoparticles:

All the glasswares used for the preparation were cleaned and soaked in freshly prepared HNO_3/HCl mixture, and rinsed thoroughly in distilled water and dried in air. For a typical preparation of gold nanoparticles of 100 ml of 330 μM concentration, aqueous solution of choloroauric acid ($HAuCl_4$) was reduced by 400 μl of freshly prepared 66 mM (2.5 mg) sodium borohydride ($NaBH_4$) in water at room temperature. The reductant was added dropwise with stirring to yield ruby red solution of gold nanoparticles (Scheme 1). The solution was subjected to ultracentrifugation and the resulting pellet was washed with double distilled water twice. The pellet was than redispersed in water for UV-VIS spectroscopy and TEM studies. For FTIR analysis, the pellet was dried and the powder was used for sample preparation.

The AuNPs were also synthesized using different concentrations of $NaBH_4$. Six sets of synthesis were done using 13.2, 26.4, 52.8, 66, 92.5 and 132 mM aqueous solution of $NaBH_4$. UV-VIS studies were done for the respective solutions.

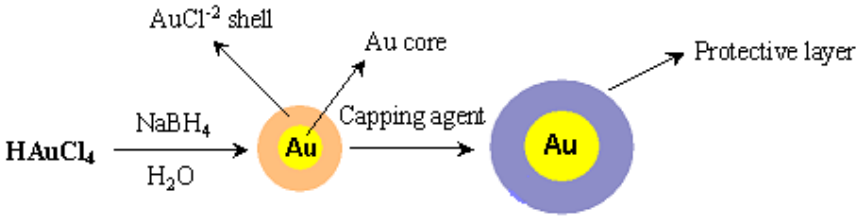

Scheme 1. Schematic representation of the synthesis and stabilization of AuNPs.

2.2.3.2 Preparation of glutathione capped AuNPs:

To the gold colloid solution prepared as stated above, the capping of gold colloid was done by the addition of 1 ml of 65 mM glutathione to 100 ml of gold solution and the mixture was stirred for 10-15 minutes. After the addition of glutathione and the mixture of gold nanoparticles solution was allowed to stand for 2 h. The solution was next subjected to centrifugation and the resulting pellet obtained was washed twice with double distilled water to remove unbound glutathione residues. The dried pellet was then used for FTIR analysis and UV-VIS spectroscopy. For further use and storage the pellet was resuspended in 0.1 M phosphate buffer (pH 7.0).

2.2.3.3 Preparation of lipoic acid capped AuNP:

Capping of gold colloid was done by the addition of 1 ml of 72 mM lipoic acid prepared in 50% aqueous ethanol to 100 ml of gold colloid and the mixture was stirred for 10-15 minutes. Gold nanoparticles were allowed to age for 2 h and the solution was subjected to centrifugation. The resulting pellet obtained was washed twice with double distilled water to remove unbound lipoic acid residues. The pellet was then used for FTIR analysis and UV-VIS spectroscopy. For further use and storage the pellet was resuspended in 0.1 M phosphate buffer (pH 7.0).

2.2.3.4 Transmission electron microscope (TEM) measurements:

Samples for TEM analysis were prepared by placing a drop of $NaBH_4$ reduced AuNPs on copper TEM grids. The film on the TEM grid was allowed to stand for 2 minutes following which, the extra solution was removed by

blotting paper and the grid was allowed to dry prior to measurement. TEM was performed at an accelerating potential at 120 kV.

2.3 Results and Discussion

2.3.1 UV-Visible spectroscopy studies of AuNPs:

The gold nanoparticles synthesized by borohydride reduction of aurate salt were relatively monodisperse in colloidal solution, which is confirmed by the TEM pictures and also by the presence of a sharp single peak in the absorbance spectra (Figure 3). The λ_{max} was observed at around 520 nm.

Figure 4 shows the UV-VIS spectra recorded as a function of time of reaction of the aurate salt reduced with $NaBH_4$ at room temperature. It was observed that, there is rapid reduction of the aqueous aurate salt ions leading to the formation of AuNPs within 5 minutes of the reaction. Upon completion of the reaction (curve 4, 15 minutes of reaction) the CV shows the formation of a well-defined surface plasmon band at ~520 nm which is characteristic of AuNPs.

2.3.2 UV-Visible spectroscopy studies of capped AuNPs:

In the next step, which involved the protection of nanoparticles for stability, we have used two different capping or protecting agents i.e., glutathione and lipoic acid. As shown in the Figure 4, the peak is shifted towards longer wavelength after capping with glutathione and lipoic acid and the λ_{max} was observed around 540-580 nm for glutathione capped and 560-620 nm for lipoic acid capped gold nanoparticles. The change in the color of the colloid was also seen before and after capping. The color of the gold colloid changed from wine red to blue for glutathione and to dark blue for

lipoic acid capped nanoparticles. This suggests the increase in size of the nanoparticles.

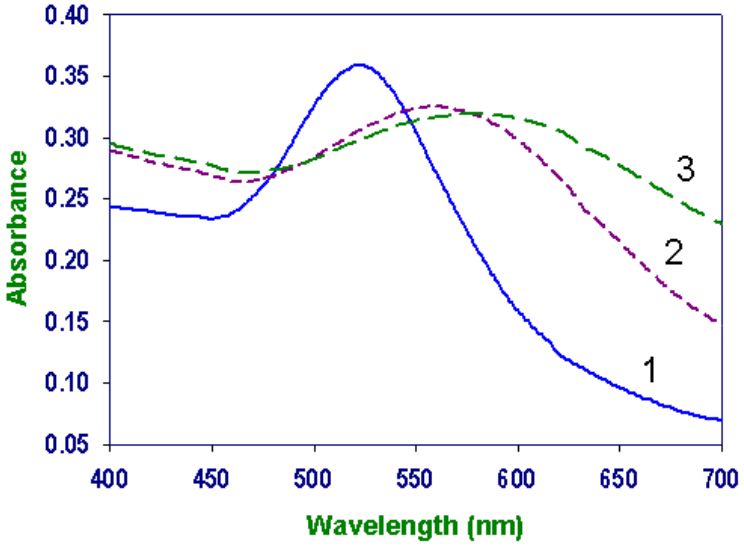

Figure. 3. UV-Visible spectrum of (1) gold nanoparticles (Au-NP), (2)glutathione capped Au-NP and (3) Lipoic acid capped Au-NP.

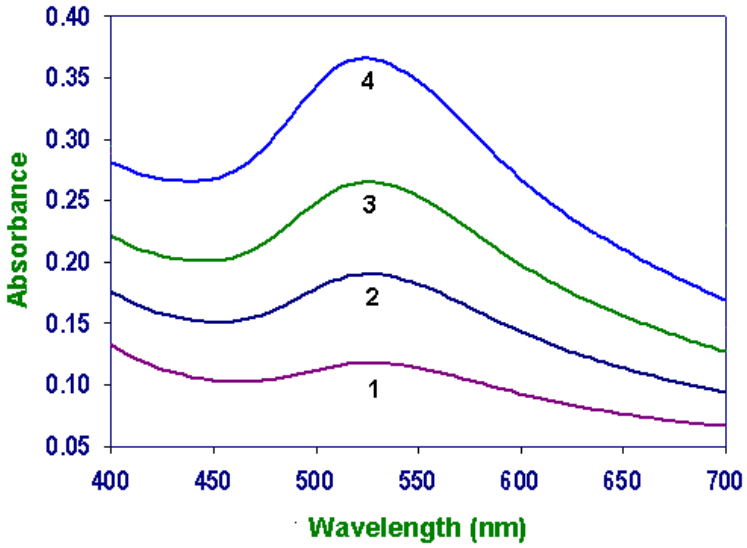

Figure. 4. UV-VIS spectrum recorded as a function of time of the reaction of aurate salt with sodium borohydride. 1: 0, 2: 5, 3: 10, 4: 15 minutes of reaction.

The λmax shift in the absorbance spectra is mainly due to the aggregation or flocculation, which is a well-understood process. This aggregation of nanoparticles was seen in both the cases of GSH and LPA capped Au-NP. The aggregation is pH dependent, after the borohydride reduction of aurate salt and the pH of the solution is increased towards the alkaline side due to negatively charged surface of nanoparticle due to the $AuCl^{2-}$ ions adsorbed onto the surface which prevents the aggregation, as glutathione or lipoic acid is added to the colloidal solution there is a change in the pH towards the acidic side due to which the change of the color is observed. In the case of glutathione capped gold nanoparticles (Figure 5A) at pH 5.0, the spectra has shifted towards the longer wavelength and as the pH is increased the shift is seen towards the lower wavelength of the spectra. Glutathione is a tripeptide (glutamic acid, cysteine and glycine) and it has many binding points towards the gold nanoparticles. There are two carboxylic groups, one thiol group and three amino groups in glutathione. These binding points are pH dependent; at alkaline pH, the carboxylic group usually remain ionized, which causes the dissociation of the carboxylic group from the gold nanoparticles resulting in low crosslinking of the nanoparticles and no aggregation is observed. At acidic pH the carboxylic group are unionized and the amino groups are ionized. The binding through α-amino group is activated and carboxylic group is suppressed which results in the crosslinking of nanoparticles and the aggregation takes place.

In the case of lipoic acid capped nanoparticles, the disulfides are reduced by borohydride to two thiol groups (–S–S– → –SH + –SH) and these thiol groups

are involved in the binding of lipoic acid to gold nanoparticles. In this type of capping, pH dependent aggregation of nanoparticles is also observed. The carboxylic group protonation at acidic pH results in the aggregation of nanoparticles and at alkaline pH the ionized carboxylic group results in well-dispersed nanoparticles. As shown in the Figure 5B at pH 7.0, the AuNPs are well dispersed and with the increasing of acidity broadening of peak is seen, which indicates the aggregation of AuNPs in the solution.

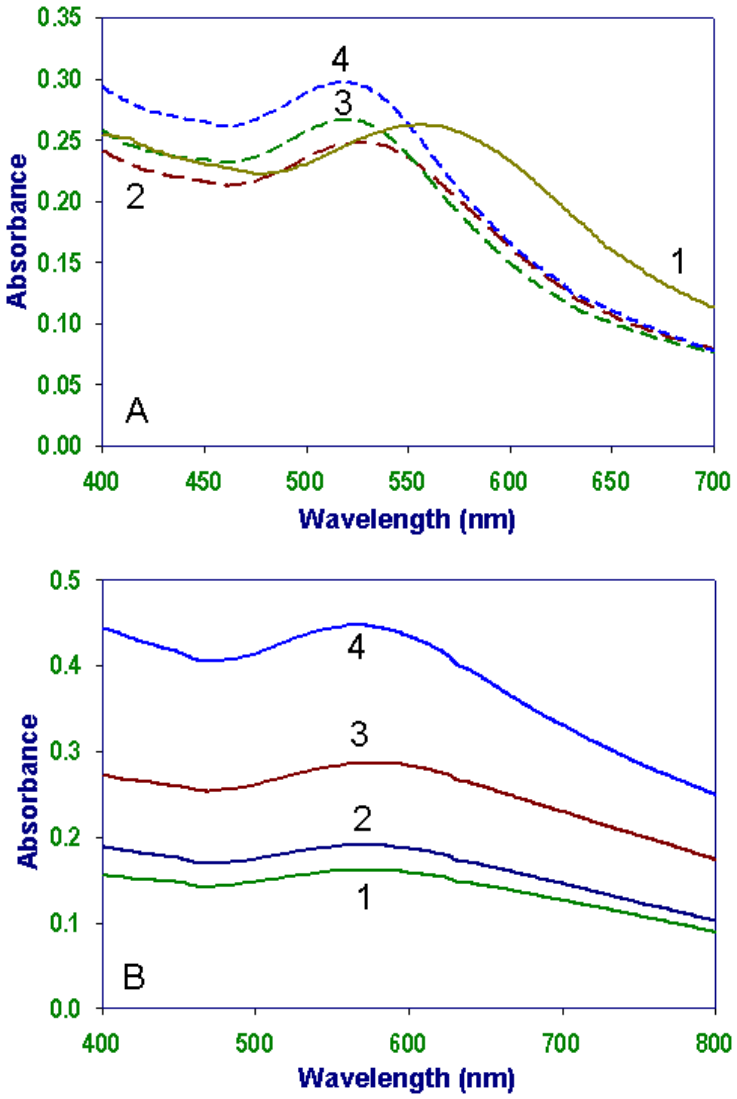

Figure. 5. UV-Visible spectrum of capped gold nanoparticles (A) glutathione capped AuNPs and (B) lipoic acid capped AuNPs in pH (1) 5.0, (2) 5.5, (3) 6.0, (4) 7.0 solutions. The pH of the solution was decreased using dilute HCl. Shift in the wavelength was observed in case of glutathione capped nanoparticles and broadening of peak was observed in case of lipoic acid capped nanoparticles.

2.3.3 Transmission electron microscope (TEM) studies:

TEM analysis of the neat (uncapped) AuNPs showed that the redispersed AuNPs are monodispersed with no sign of any significant aggregation. The individual AuNPs at higher magnification in the TEM image showed that the particles are evenly round shape and the average size of the AuNPs is around ~25 nm, indicating that the nanoparticles are water dispersible and quite stable in aqueous solution (Figure 6).

2.3.4 Fourier transform infrared (FTIR) spectroscopy studies of AuNPs:

FTIR measurements were carried out to study the binding of glutathione and lipoic acid to neat gold nanoparticles (Figures 7a), glutathione (Figure 7b), lipoic acid (Figure 7d) and gold nanoparticles capped with glutathione (Figure 7c) and lipoic acid (Figure 7e) shows the FTIR spectra respectively

We note that after coupling to the gold nanoparticles, a number of peaks present in the free molecules (Figure 7b: peaks at 549 cm^{-1}, probably S-S stretch, and 2,525 cm^{-1}, probably S-H stretch; Figure 7d: 671 cm^{-1} and 518 cm^{-1}, probably S-S stretch) practically disappear (Figure 7c, 7e). Characteristic frequencies for the peptide bond are not significantly affected (Figure 7b: 3,128 cm^{-1} and 3,032 cm^{-1}; Figure 7c: 3,271 cm^{-1}; Figure 7d: 1,657 cm^{-1} and 1,541 cm^{-1}; Figure 7e: 1,666 cm^{-1} and 1,626 cm^{-1}), as expected (Table 1). We suggest that the vibrations are quenched or shielded by the gold nanoparticles and the energy is transferred to the internal modes of the nanoparticles. One of the reasons may be that the molecules which are attached to the nanoparticles

on the side of IR source are getting absorbed and the vibrational energy is not transmitted to the detector, whereas the molecules on the other side of the nanoparticles are getting transmitted but the vibrational energy is not sufficient to be detected. The S-S stretch vibration disappears completely in glutathione after coupling and S-H stretch vibration disappears completely in lipoic acid after coupling. A few vibrational modes survive and can still be seen in the FTIR spectrum of the coupled gold nanoparticles. Loss of S-H and S-S stretches may likely to be indicated by the covalent attachment of the respective molecules

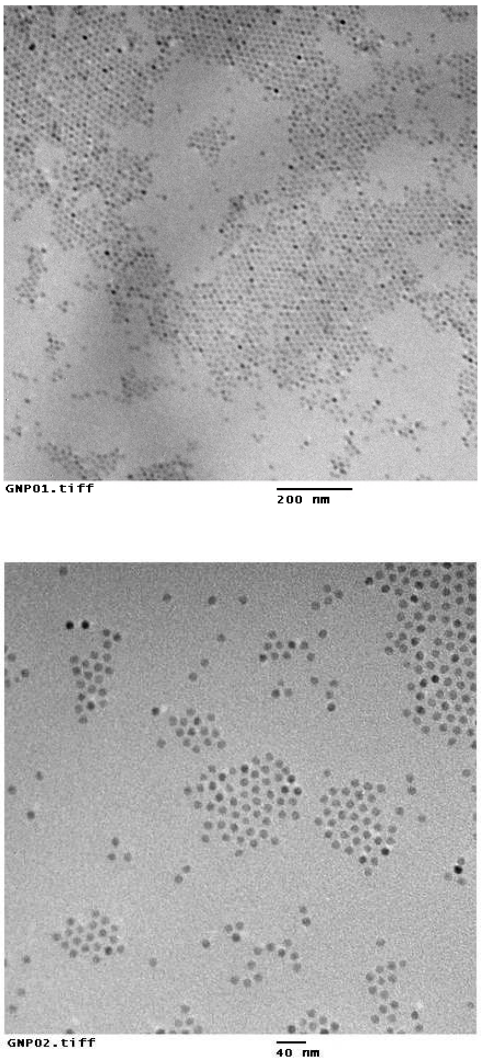

Figure. 6. TEM image of monolayer film of synthesized gold nanoparticles using sodium borohydride reduction method. Accelerating potential at 120 kV. The figure shows the images of gold nanoparticles at two different scales (200 and 40 nm).

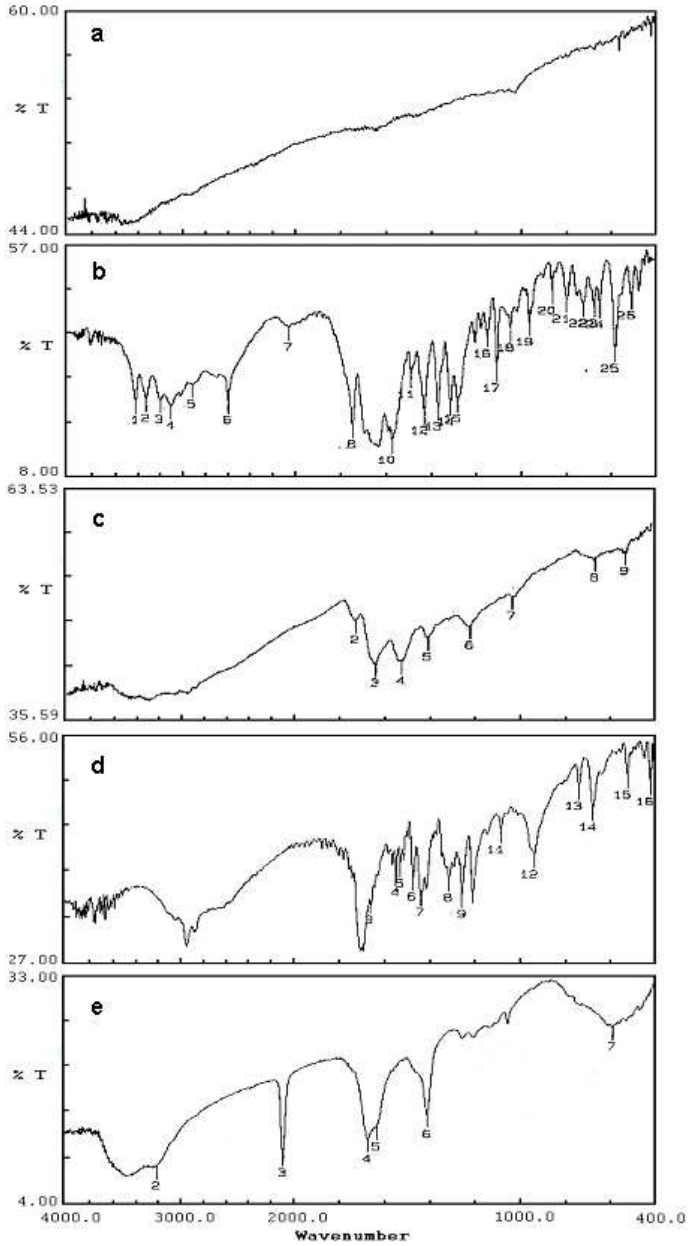

Figure. 7. FT-IR (JASCO FT/IR-5300) spectrum in KBr mulls of (a) gold nanoparticles, (b) glutathione powder and (c) gold nanoparticles capped with glutathione, (d) lipoic acid powder, (e) gold nanoparticles capped with lipoic acid. After coupling with gold nanoparticles, weak signal virtually disappear, perhaps due to the lower concentration, but several stronger peaks survive.

Table. 1. Frequencies calculated from the FTIR spectra of glutathione, glutathione capped, lipoic acid and lipoic acid capped AuNPs

Figure	Wave number	Origin
b	2525 cm^{-1}	S-H stretch
d	671 cm^{-1} and 518 cm^{-1}	S-S stretch
Practically disappears in figure c and f		
c, e	3128cm^{-1} and 3271cm^{-1}	O-H stretch
c	1657cm^{-1} and 1541 cm^{-1}	N-H stretch
Characteristic vibration of amine and hydroxy groups are not significantly changed and suggests that they are not affected.		

2.3.5 Determination of size of AuNPs from UV-Vis spectra:

Two equations (equation 1 and 2) were provided from the reference (Haiss *et al*., 2007) for calculating the size of the AuNPs using the spectroscopy. One is equation applied to nanoparticles greater than 35 nm in diameter, the other for gold nanoparticles 5 to 30 nm in diameter and the equation 1 for the smaller gold nanoparticles can be attributed to a pronounced increase of the ratio of surface atoms to bulk atoms.

$$d = \frac{\ln\left(\frac{\lambda_{spr} - \lambda_0}{L_1}\right)}{L_2} \qquad \text{(Equation 1)}$$

Where d is the diameter of the AuNPs, λ_{spr} is the wavelength at the peak of the surface plasmon resonance (SPR), $\lambda_0 = 512$, $L_1 = 6.53$, and $L_2 = 0.0216$. Haiss finds an absolute error of 3%.

To calculate the diameter of our AuNPs for sizes 5 to 30 nm, we use another Haiss equation (Equation 2):

$$d = \left(\frac{A_{spr}\left(5.89X10^{-6}\right)}{c_{Au}\exp\left(C_1\right)} \right)^{\frac{1}{C_2}} \qquad \text{(Equation 2)}$$

Where A_{spr} is the absorbance (AU) at the peak SPR, C_{Au} (moles/L) is the amount of gold used in the synthesis, C_1 = -4.75, and C_2 = 0.314. The error calculated by Haiss is ~ 6%.

AuNPs were prepared by borohydride reduction method stated earlier (2.2.3.1). Six set of synthesis was done using different amount of $NaBH_4$ 5.0, 3.5, 2.5, 2.0, 1.0 and 0.5 mg. The respective spectra (Figure 8) were taken and the size was calculated using the above equation (Table 2).

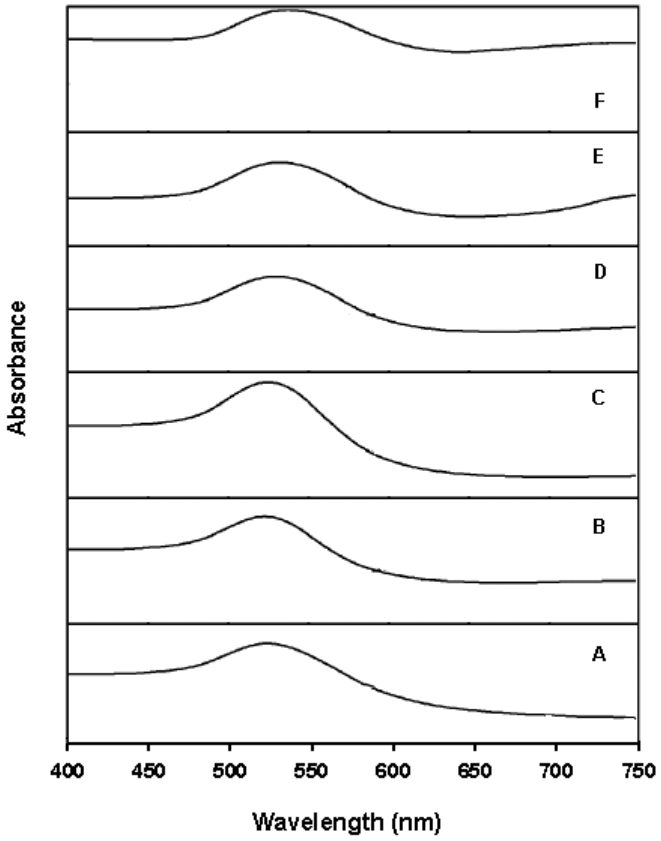

Figure. 8. UV-VIS spectrum of AuNPs synthesized using different concentrations $NaBH_4$. Where the aurate salt concentration was constant 300 µM (10 $mgmL^{-1}$) and the $NaBH_4$ concentration in set (A) 132.1 µM, (B) 92.5 µM, (C) 66 µM, (D) 52.8 µM, (E) 26.4 µM, (F) 13.2 µM.

Table. 2. Average size of AuNPs synthesized using different amount of sodium borohydride calculated using Haiss equation

Set	$HAuCl_4$ (mg/100mL)	$NaBH_4$ (mM)	Color	λ_{max}	Average diameter of nanoparticles calculated (nm)
A	10	132.1	Pink	514	10
B	10	92.5	Pink	516	16
C	10	66	Pink	519	20
D	10	52.8	Red	520	25
E	10	26.4	Red	523	30
F	10	13.2	Red	532	38

Based on the spectra and the calculated size, we have seen that by controlling the amount or the concentration of the reducer the size of the nanoparticles can be changed.

2.4 Conclusions

We have demonstrated the synthesis and capping of gold nanoparticles using two different capping agents, glutathione and lipoic acid, the capping of gold nanoparticles lead to water dispersible nanoparticles which can be used for further modifications. The capping was confirmed by UV-VIS spectroscopy and FTIR studies. The UV-VIS spectroscopy studies showed that after the capping of gold nanoparticles, there was a shift in the wavelength from 520nm (specific plasmon resonance for gold nanoparticles) towards longer wavelength for both the glutathione and lipoic acid capped nanoparticles. From TEM analysis, we observed that the nanoparticles were evenly shaped with no sign of aggregation. The average size of the nanoparticles was around ~20nm which agrees well with the theoretical calculation using UV-VIS spectroscopy.

2.5 References

- Amirkin, C.; Letsinger, R.L.; Mucic, R.C.; Sterhoff, J.J. (1996). A DNA based method for rationally assembling nanoparticles into macroscopic materials. *Nature*, 382, 607-609.
- Aslam, A.; Fu, L.; Su, M.; Vijayamohanan, K.; Dravid, V.P. (2004). Novel one-step synthesis of aminestabilized aqueous colloidal gold nanoparticles. *J. Mater. Chem.,* 14, 1795-1797.
- Authier, L.; Grossiord, C.; Brossier, P. (2001). Gold nanoparticle-based quantitative electrochemical detection of amplified human cytomegalovirus DNA using disposable microband electrodes. *Anal. Chem*., 73, 4450-4456.
- Basu, S.; Pal, T. (2007). Glutathione-induced aggregation of gold nanoparticles: electromagnetic interactions in a closely packed assembly, *J. Nanosci. Nanotechnol*., 7, 1904
- Brust, M.; Fink, F.; Bethella, D.; Schiffrina, D.J.; Kiely, C. (1995). Synthesis and reactions of functionalised gold nanoparticles. *J. Chem. Soc., Chem. Commun*., 1655-1656.
- Brust, M.; Walker, M.; Bethell, D.; Schiffrin J.D.; Whyman, R. (1994). Synthesis of thiol-derivatised gold nanoparticles in a two-phase liquid-liquid system. *J. Chem. Soc., Chem. Commun*., 801-802.

- Burt, J.L.; Wing, C.G.; Yoshida, M.M.; Yacama, M.J. (2004). Noble-Metal nanoparticles directly conjugated to globular proteins. *Langmuir*, 20, 11778-11783.
- Castaneda, M.T.; Alegret, S.; Merkoci, A. (2007). Electrochemical sensing of DNA using gold nanoparticles. *Electroanalysis*, 19, 743-753.
- Cai, H.; Xu, C.; He, P.; Fang, Y. (2001). Colloid Au-enhanced DNA immobilization for the electrochemical detection of sequence-specific DNA. *J. Electroanal. Chem*., 510, 78-85.
- Daniel, M, C., Astruc, D. (2004). Gold nanoparticles: assembly, supramolecular chemistry, quantum-size-related properties, and applications toward biology, catalysis, and nanotechnology. *Chem. Rev*., 104, 293–346.
- Dequaire, M.; Degrand, C.; Limoges, B. (2000). An electrochemical metalloimmunoassay based on a colloidal gold label. *Anal. Chem*., 72, 5521-5528.
- Dua, D.; Liub, S.; Chena, J.; Jua, H.; Liana, H.; Lia, J. (2005). Colloidal gold nanoparticle modified carbon paste interface for studies of tumor cell adhesion and viability. *Biomaterials*, 26, 6487-6495.
- Fitzmaurice, D., Connolly, S. (1999). Programmed assembly of gold nanocrystals in aqueous solution. *Adv.Mater*., 11, 1202–1205.

- Gole, A.; Dash, C.; Soman, C.; Sainkar, S.R.; Rao, M.; Sastry, M.(2001). On the preparation, characterization, and enzymatic activity of fungal protease gold colloid bioconjugates. *Bioconjugate Chem*., 12, 684-690.
- Haiss, W., Thanh, N. T K., Avegard, J., Fernig, D. (2007). Determination of size and concentration of gold nanoparticles form UV-VIS spectra. *Anal chem.*, 79 (11), 4215-4221.
- Hua, S.Q.; Xie, J.W.; Xu, Q.H.; Rong, K.T.; Shen, G.L.; Yu, S.Q. (2003). A label-free electrochemical immunosensor based on gold nanoparticles for detection of paraoxon. *Talanta*, 61, 769-777.
- Hu, S.Q.; Xie, J.W.; Xu, Q.H.; Rong, K.T.; Shen, G.L.; Yu, R.Q. A (2003). Label-free electrochemical immunosensor based on gold nanoparticles for detection of paraoxon. *Talanta*, 61, 769-777.
- Ju, H.; Liu, S.; Ge, B.; Lisdat, F.; Scheller, F.W. (2002). Electrochemistry of cytochrome c immobilized on colloidal gold modified carbon paste electrodes and its electrocatalytic activity. *Electroanalysis*, 14,141-147.
- Kreibig, U., Vollmer, M. (1995). Optical Properties of Metal Clusters; Springer Series in Material Science, No. 25; Springer-Verlag: Berlin, 187–201.
- Kumar, S.; Aaron, J.; Sokolov, K. (2008). Directional conjugation of antibodies to nanoparticles for synthesis of multiplexed optical

contrast agents with both delivery and targeting moieties. *Nat.Protoc*., 3, 314-320.

- Kumar, S.; Aaron, J.; Sokolov, K. (2008). Directional conjugation of antibodies to nanoparticles for synthesis of multiplexed optical contrast agents with both delivery and targeting moieties. Nat.protoc., 3, 314-320.
- Li, X.; Yuan, R.; Chai, Y.; Zhang, Z.; Zhuo, Y.; Zhang, Y. (2006). Amperometric immunosensor based on toluidine blue/nano-Au through electrostatic interaction for determination of carcinoembryonic antigen. *J. Biotechnol*., 123, 356-366.
- Liu, S.; Ju, H. (2003). Electrocatalysis via direct electrochemistry of myoglobin immobilized on colloidal gold nanoparticles, *Electroanalysis*, 15,1488-1493.
- Motesharei, K., Myles, D, C. (1994). Molecular recognition in membrane mimics: A fluorescence probe. *J. Am.Chem. Soc*., 116, 7413–7414.
- Mirkin, C, A., Taton, T, A. (2000). Materials chemistry: Semiconductors meet biology. *Nature*, 405, 626–627.
- Mann, S., Shenton, W., Li, M., Connolly, S., Fitzmaurice, D. (2000). Biologically programmed nanoparticles assembly. *Adv. Mater*., 12, 147–150.

- Parak, W.J.; Gerion, D.; Pellegrino, T.; Zanchet, D.; Micheal, C.; Williams, S.C.; Boudreau, R.;Gros, M.AL.; Larabell, C.A.; Alivisatos, A.P. (2003). Biological applications of colloidal. *Nanocrystals. Nanotechnology*, 14, R15–R27.

- Porta, F.; Speranza, G.; Krpeti, Z.; Santo, V.D.; Francescato, P. (2007). Gold nanoparticles capped by peptides. *Mater. Sci. Eng., B*, 140,187-194.

- Sastry, M., Lala, N., Patil, V., Chavan, S, P., Chittiboyina, A, G. (1998). Optical absorption study of the biotin-avidin interaction on colloidal silver and gold particles. *Langmuir*, 14, 4138–4142.

- Storhoff, J.J.; Elghanian, R.; Mucic, R.C.; Mirkin, C.A.; Letsinger, R.L. (1998). One-Pot colorimetric differentiation of polynucleotides with singlebase imperfections using gold nanoparticle probes. *J. Am. Chem. Soc*., 120, 1959-1964.

- Subramaniam, C.; Tom, R.T.; Pradeep, T. (2005). On the formation of protected gold nanoparticles from $AuCl_4^-$ by the reduction using aromatic amines. *J. Nanopar. Res*., 7, 209-217.

- Tkachenko, A.G.; Xie, H.; Coleman, D.; Glomm, W.; Ryan, J.; Anderson, M.F.; Franzen, S.;Feldheim, D.L. (2003). Multifunctional Gold nanoparticle-peptide complexes for nuclear targeting. *J. Am.Chem. Soc*., 125, 4700-4701.

- Tang, H.; Chena, J.; Nie, L.; Kuang, Y.; Yao, S. (2007). A label-free electrochemical immunoassay for carcinoembryonic antigen (CEA) based on gold nanoparticles (AuNPs) and nonconductive polymer film. *Biosens. Bioelectron*., 22, 1061-1067.

- Tkachenko, A.G.; Xie, H.; Coleman, D.; Glomm, W.; Ryan, J.; Anderson, M.F.; Franzen, S.; Feldheim, L. (2003). Multifunctional Gold Nanoparticle-Peptide Complexes for Nuclear Targeting. *J. Am Chem. Soc*., 125, 4700-4701.

- Warner, M. G., M, G., Hutchison, J, E. (2003). Synthesis, Functionalization and Surface Treatment of Nanoparticles (Ed. M.-I. Baraton), American Scientific Publishers: Stevenson Ranch, California, Chapter 5, 67.

- Wang, H.; Chen, Y.; Li, W.Y.; Liu, Y. (2007). Synthesis of oligo (ethylenediamino)-β-cyclodextrin modified gold nanoparticle as a DNA concentrator. *Mol. Pharm*., 4, 189-198.

- Wang, L.; Wei, G.; Sun, L.; Liu, Z. (2006). Self-assembly of cinnamic acid-capped gold nanoparticles. *Nanotechnology*, 17, 2907-2912.

- Yi, X.; Xian, J.H.; Yuan, C.H. (2000). Direct electrochemistry of horseradish peroxidase immobilized on a colloid/cysteamine-modified gold electrode. *Anal. Biochem*., 278, 22-28.

- You, C.C.; De, M.; Han, G.; Rotello, V.N. (2005). Tunable inhibition and denaturation of α-Chymotrypsin with Amino Acid-Functionalized Gold Nanoparticles. *J. Am. Chem. Soc*., 127, 12873-12881.
- Yonezawa1, T.; Nomura, T.; Kinoshita, T.; Koumoto, K. (2006). Preparation and characterization of polypeptide stabilized gold nanoparticles. *J. Nanosci. Nanotechnol*., 6, 1649-1650.
- Zheng, M.; Davidson, F.; Huang, X. (2003). Ethylene glycol monolayer protected nanoparticles for eliminating nonspecific binding with biological molecules. *J. Am. Chem. Soc*., 125, 7790-7791.

Chapter 3

Direct Electrochemistry of Horseradish Peroxidase - Gold Nanoparticles Conjugate

3.1 Introduction

The performance of biosensors depends greatly on proper and efficient immobilization of biomolecule. In this context the use of nanoparticles for the construction of sensing devices has been increased. The use of gold nanoparticles (AuNPs) for the construction of electrochemical biosensors (Jose *et al*., 2008) allows enhancement of the analytical performance with respect to other designs.

The ability of AuNPs to provide a stable immobilization of biomolecules (DNA, proteins and enzymes) retaining their bioactivity is a major advantage in the preparation of biosensor transducers. AuNPs being metallic in nature permit direct electron transfer between redox proteins and the bulk electrode materials. This allows electrochemical sensing to be performed with no need of electron transfer mediators. One of the important features of AuNPs, shared by all nanoparticles, is their high surface to volume ratio, which helps in faster reaction and greater protein load. And the other ability is to decrease the protein-metal particles distance and function as electron conducting pathway between the prosthetic groups and the electrode surface.

- **Horseradish Peroxidase (HRP):**

The capped gold nanoparticles are used in the coupling of biomolecules, as they have suitable functional groups. One of the common and suitable enzyme, which can be used for this coupling is horseradish peroxidase (HRP). HRP has been used for the construction of biosensor, for the determination of H_2O_2 and small organic peroxides and for the sensing of glucose, alcohol and

other analytes, because of its relatively small size and high chemical and thermal stability. Peroxidases are enzymes of the EC 1.11.1.7 class, which are defined as oxidoreductases that use hydroperoxides as electron acceptor. It has been found that peroxidases such as plant peroxidases, cytochrome c peroxidase, chloroperoxidase, lactoperoxidase etc, are all heme proteins with a common catalytic cycle (Ruzgas *et al*., 1996) (Scheme 1). HRP is a globular glycoprotein with a mass of 42 kDa, of which the protein moiety is approximately 34 kDa, the rest of the molecular weight being accounted for by the prosthetic group (b-type heme), two calcium ions and some surface bound sugars (Figure 1). The enzyme shows a characteristic Soret band at 402 nm due to the presence of heme in it, which is often used for the determination of the purity of the enzyme.

The physical properties of HRP has been studied as follows (Mehly, 1995),

- Molecular weight: 40 kDa.
- Isoelectric point: 7.2.
- Solubility: 5 grams of enzyme is soluble in 100 mL of water if traces of salts are present. In ammonium sulphate precipitation, the enzyme is soluble upto 58% (w/w) but insoluble above 62% (w/w).
- PH stability: The enzyme is stable in the pH range of 5 to 12. The activity is terminated below pH 3.5. The pH optimum of HRP is in the range of 6.0 to 6.5.

- Thermal stability: The enzyme is stable for weeks at room temperature. However at higher temperature it has been reported to be stable upto $63^{o}C$ for 15 minutes (Mehly, 1995).

- Oxidation-Reduction potentials: The redox potential of the enzyme was determined (Harbury, 1957) and was found to be at $E^{o`}$ -207 mV at pH 6.08 and $E^{o`}$ -278.7 mV at pH 7.7.

- Substrate specificity: The substrate specificity of HRP in forming Compound-I is high. Hydrogen peroxide (H_2O_2), Methyl hydrogen peroxide and Ethyl hydrogen peroxide are the only compounds that could combine with HRP to form the active substrate complex Compound-I (Maehly, 1995, Chmeilnicka, 1971 and Morrisson, 1973). However the specificity of the enzyme substrate complexes for hydrogen or electron donors (AH) is quite low. Hence AH (Scheme 1) represents a number of different compounds such as 4-aminoantipyrene, cytochrome c, ferrocyanide, phenols, amino phenols, diamines, indophenols, ascorbic acid, leucodyes and some amino acids.

- Inhibitors: HRP is reversibly inhibited by cyanide and sulfide at concentration of 10.5 M (Theorell, 1951).

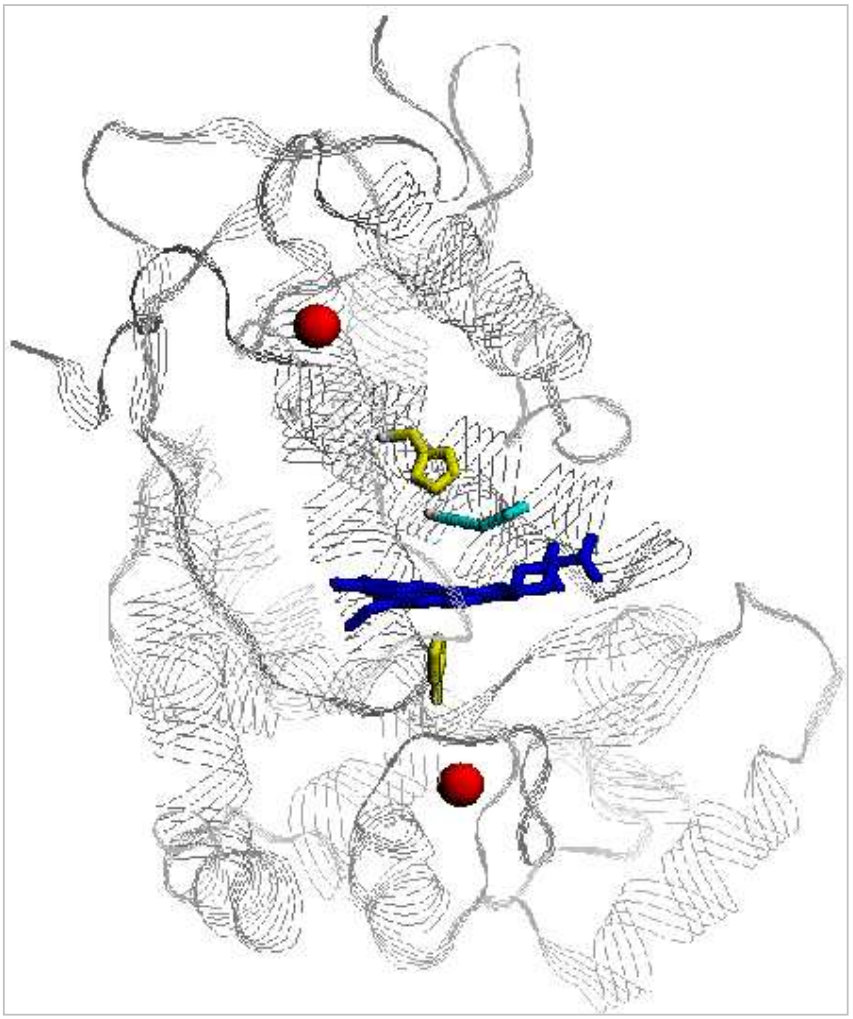

Figure 1. The HRP structure: Shown are the heme (blue), the essential calcium ions (red), and the three key aminoacid residues: the proximal (below the heme) and distal (above the heme) histidines (yellow) and the distal pocket arginine (cyan). RCSB PDB J. Mol. Viewer. PDB ID: 1HCH (Berglund).

HRP catalyzes the oxidation of a number of electron donors such has ascorbate, feroocyanide, cytochrome C and leuco forms of many dyes through H_2O_2 as the electron acceptor.

3.1.1 Reaction mechanism of HRP:

The reaction mechanism of HRP has been extensively studied (Shannon *et al*., 1966, Mehly, 1955, Chance, 1951, Dawson *et al*., 1988). The studies have shown that the HRP works in three steps as seen in Scheme 1 and Figure 2.

$$\text{Native peroxidase [Fe (III)]} + H_2O_2 \longrightarrow \text{Compound-I} + H_2O \quad (1a)$$

$$\text{Compound-I} + AH_2 \longrightarrow \text{Compound-II} + AH^* \quad (1b)$$

$$\text{Compound-II} + AH_2 \longrightarrow \text{Native peroxidase [Fe (III)]} + AH^* + H_2O \quad (1c)$$

Scheme 1. The reactions in the enzymatic catalytic cycle of HRP

The first step in (scheme 1:la) involves the two-electron oxidation of the ferriheme prosthetic group of the native peroxidase by H_2O_2 (or an organic hydroperoxides). This reaction results in the formation of an intermediate, compound-I (oxidation state +5), consisting of oxyferryl iron (Fe (IV) O=0) and a porphyrin π cation radical. In the next reaction (1b), compound-I (Maehly *et al*., 1954, Chmielnicka *et al*., 1971) loses one oxidizing equivalent upon one-electron reduction by the first electron donor AH_2 and forms compound-II (oxidation state +4). The later in turn accepts an additional electron from the second donor molecule AH_2 in the third step (lc), whereby the enzyme is returned to its native resting state, ferriperoxidase. The overall charge on the resting state and the compound-I is +1.

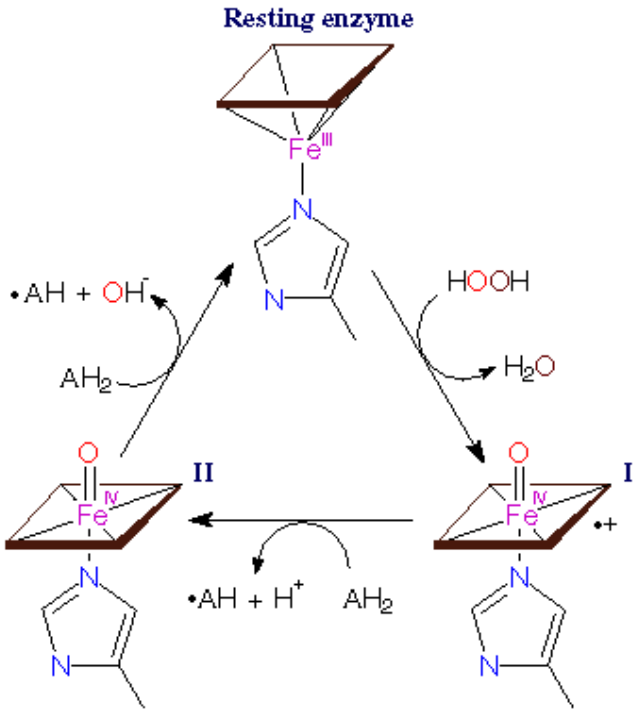

Figure 2. Peroxidase catalyzed oxidative reactions scheme using hydrogen peroxide as the electron acceptor (metallo scripps).

Direct electrochemistry has been observed for the adsorbed peroxidase. There was a registered reduction in the current and peroxide concentration that was observed in gold, graphite and platinum. The electrode current was found due to an electrochemical reduction of compound-I and compound-II as schematically presented in Figure 3 below.

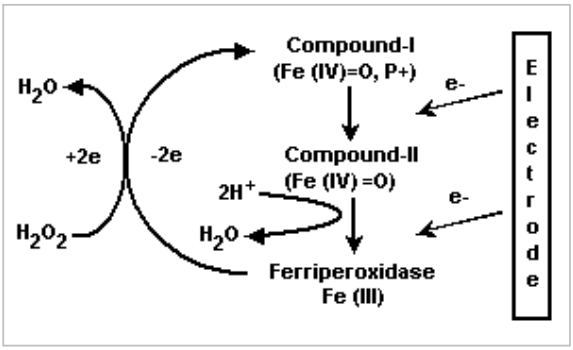

Figure 3. Mechanism of the direct bioelectrocatalytic reduction of hydrogen peroxidase at peroxidase-modified electrodes. P^+ is a cation radical localized on the porphyrin ring or polypeptide chain.

The direct assembly of monolayer HRP onto the metal surface often results in the denaturation and significant loss of enzyme activity. Earlier workers have reported the use of AuNPs modified electrodes for immobilizing the enzyme, by using layer by layer enzyme assembly (Gao *et al*., 2007, Yu *et al*., 2008, Liu *et al*., 2006, Wang *et al*., 2005, Luo *et al*., 2008), entrapping the enzyme in a silica sol gel (Di *et al*., 2005, Jia *et al* 2002), by electrostatic interactions (Xiang *et al*., 2008), and by using a carbon paste electrode (Liu *et al*., 2002).

In this work we describe a new approach for the development of sensors by directly linking the HRP to the AuNPs by using the crosslinker carbodiimide, which forms an amide bond between the carboxylic group of capped AuNPs and amino groups present in the HRP. In this way, the enzyme is freely

available in the solution while attached to the AuNPs with a short linker. This approach allows the substrate to approach the enzyme without encountering steric hindrance from the AuNPs. This process is a simple and stable method for enzyme immobilization. The HRP was linked to both the glutathione and lipoic acid capped AuNPs and immobilized onto the gold electrodes to study the electrochemical properties. The linker can be lengthened by a simple modification of this protocol for the other enzymes/proteins.

3.2 Materials and methods

3.2.1 Materials and instrumentation:

For the present study, we have used HRP (EC 1.11.1.7. RZ ~3, >250u/mg) and *N*-Ethyl-*N*′-(3-dimethylaminopropyl) carbodiimide hydrochloride (EDC), Choloroauric acid ($AuCl_4.4H_2O$) (Au% > 49%) were purchased from Sigma. All other chemicals were of the analytical grade and were used without further purification. All the solutions were prepared using double distilled water.

The absorption spectrum of the samples was recorded in UV-1601 spectrophotometer (Shimadzu). Electrochemical measurements were performed using CHI 660A electrochemical workstation (CH Instruments, USA) with conventional three electrode system, comprising of platinum auxiliary electrode, an Ag/AgCl reference electrode and a gold electrode (as the working electrode). The 1:1 ratio of 0.1M phosphate buffer (PB) pH 7.2 and 0.1M KCl was used as electrolyte for all the measurements. All the potentials reported here refer to the Ag/AgCl (sat. KCl) reference electrode.

3.2.2 Synthesis of sodium borohydride reduced gold nanoparticles:

All the glassware's used for the preparation were cleaned and soaked in freshly prepared HNO_3/HCl mixture, and then they were rinsed thoroughly in distilled water and dried in air. In a typical preparation of gold nanoparticles a quantity of 100 ml of 330 μM concentrated aqueous solution of choloroauric acid ($HAuCl_4$) was reduced by 400 μl of freshly prepared 66 mM sodium borohydride ($NaBH_4$) aqueous solution at room temperature. The reductant

was added dropwise with stirring to yield a ruby red color solution of gold nanoparticles (Scheme 2). The solution was subjected to ultracentrifugation at 25000 rpm and the resulting pellet was washed with double distilled water twice. The pellet was than redispersed in water for UV-VIS spectroscopy studies and TEM analysis. For FTIR analysis the pellet was used for sample preparation.

3.2.3 Preparation of glutathione capped AuNPs:

To the gold colloid solution prepared as stated above, the capping was done by the addition of 1 ml of 65 mM of glutathione to 100 ml of gold solution and the mixture was stirred for 10-15 minutes. After the addition of glutathione and aging of the gold nanoparticles solution for 2 h, the solution was subjected to centrifugation and the resulting pellet obtained was washed twice with double distilled water to remove unbound glutathione residues. The pellet was resuspended in 0.1 M phosphate buffer (pH 7.2) and used for UV-VIS spectroscopy studies and was stored for further analysis. The dried pellet was then used for FTIR.

3.2.4 Preparation of lipoic acid capped AuNPs:

To the gold colloid solution prepared as stated above, the capping was done by the addition of 1 ml of 72 mM of lipoic acid prepared in ethanol: water (1:1 ratio) to 100 ml of gold solution and the mixture was stirred for 10-15 minutes. After the addition of glutathione and aging of the gold nanoparticles solution for 2 h, the solution was subjected to centrifugation and the resulting pellet obtained was washed twice with double distilled water to

remove unbound lipoic acid residues. The pellet was resuspended in 0.1 M phosphate buffer (pH 7.2) and used for UV-VIS spectroscopy studies and was stored for further analysis. The dried pellet was then used for FTIR.

3.2.5 Preparation of HRP-AuNPs conjugate:

The covalent coupling process using EDC generally involves two steps, one is activation of the carboxylic acid group, and this step is carried out at slightly acidic pH 4.5-5.0. The second step involves the amide bond formation between the activated carboxylic groups of one species with the amino group of the other and can be carried out at basic pH (Scheme 2).

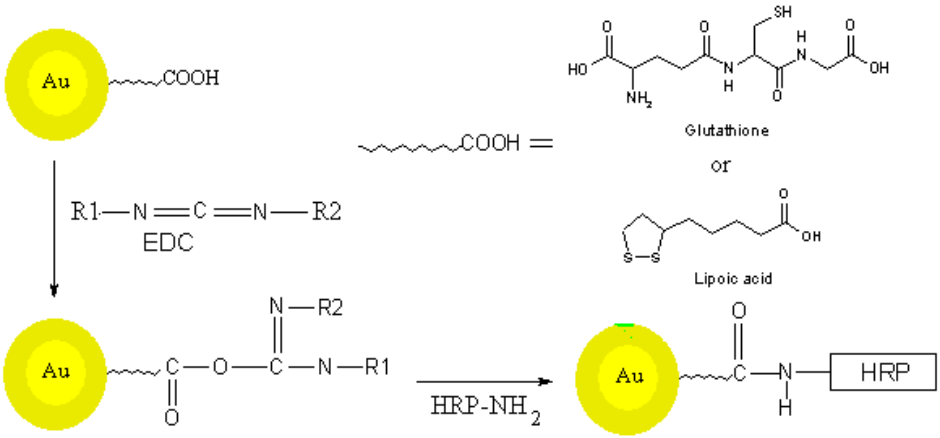

Scheme 2. Schematic representation of the covalent coupling of HRP to capped AuNPs.

3.2.5.1 Steps involved in the covalent linking of HRP to AuNPs:

(i) Activation of carboxylic groups in AuNPs:

Both glutathione and lipoic acid capped AuNPs were used as separate sets for the linking of HRP in independent experiments. The carboxylic groups present in the glutathione and lipoic acid were activated by EDC. The capped AuNPs (0.5 mg) were dissolved in pH 5.0 MES buffer (3 mL) and 58 mM EDC (300 µL) was added and the reaction mixture was kept at 4^{o}C for 1.5 h on a rocker. After the reaction has completed, the mixture was centrifuged at 15,000 rpm for 1 h to separate the activated AuNPs from the unreacted EDC. The pellet obtained was than washed with water twice and resuspended in the MES buffer.

(ii) Covalent linking of HRP with activated AuNPs:

To the activated AuNPs suspension (1 mL), 150 µL of HRP (3 mg/mL in water) was added and the reaction mixture was kept at 4^{o}C overnight. After the reaction time the resulting HRP-AuNPs conjugate was centriguged at 4500 rpm to separate the conjugate and the pellet was dissolved in phosphate buffer.

(iii) HRP enzyme assay:

The activity of the HRP-AuNPs conjugate was performed using purpurogallin method. This method measures the oxidation of pyrogallol to purpurogallin in the presence of hydrogen peroxide by peroxidase when catalyzed by the enzyme at 420 nm.

3.2.6 Preparation of HRP-AuNPs film:

The modified electrode was prepared by putting HRP-AuNPs conjugate (5 μL) onto the cleaned and polished gold electrode and allowing it to dry at room temperature. After drying the electrode was rinsed with phosphate (pH 7.2) buffer and used for the electrochemical measurements.

3.2.7 Measurement procedure:

The HRP-AuNPs modified electrode was than placed in electrochemical cell containing 2.0 mL of 0.1 M PB (pH 7.2) and 0.1 M KCl. 10 mM of H_2O_2 was used as substrate. The cyclic Voltammetry measurements were done at the potential range of 0.40 V to 0.10 V for glutathione capped AuNPs-HRP electrode and 0.20 V to 0.10 V for lipoic acid capped AuNPs-HRP electrode at a scan rate of 10 mV/s and Ag/AgCl as the reference electrode. All the electrochemical measurements were performed at room temperature.

3.3 Results and Discussions

3.3.1 Electrochemical studies of HRP coupled to AuNPs:

The capped AuNPs were used for studying the binding properties of the AuNPs to the proteins. For this study we have used horseradish peroxidase (HRP) and used cyclic voltammetry to study the electrochemistry. HRP was covalently linked to both glutathione and lipoic acid capped AuNPs using carbodiimide coupling agent.

3.3.2 Electrochemical studies of HRP coupled capped AuNPs:

The cyclic voltammogram of 10.2 μM H_2O_2 in pH 7.2 phosphate buffer at gold modified electrode with HRP labeled gold nanoparticles showed a well defined redox peaks for the HRP (Fe(IV)/HRP(Fe(III)) redox couple transformation (Figure 4). This redox couple can be ascribed to the direct electron transfer between the HRP and the underlying electrode surface and was observed only at HRP coupled to glutathione and lipoic acid capped AuNPs. The cathodic (E_{pc}) and anodic (E_{pa}) peak potential were located at the potential 0.110V and 0.182V for HRP coupled to glutathione capped AuNPs, 0.011V and 0.089V for lipoic acid capped AuNPs respectively. The blank cyclic voltammogram showed no redox peaks. Both the modified electrodes showed good response towards the reduction of H_2O_2 as the peak separation value ΔEp was ~39 mV. The direct electron transfer reaction between the cofactor of HRP and the electrode surface was due to the favored orientation of HRP molecule or gold NP acting as the conducting channels for the electron transfer. Other workers have reported significantly different potentials

(Epa ~ 160 mV and Epc ~190 mV) using glassy carbon (which often shows high overpotential to electron transfer) as the base electrode. Our results are closer to 0 mV suggesting a more efficient electron transfer.

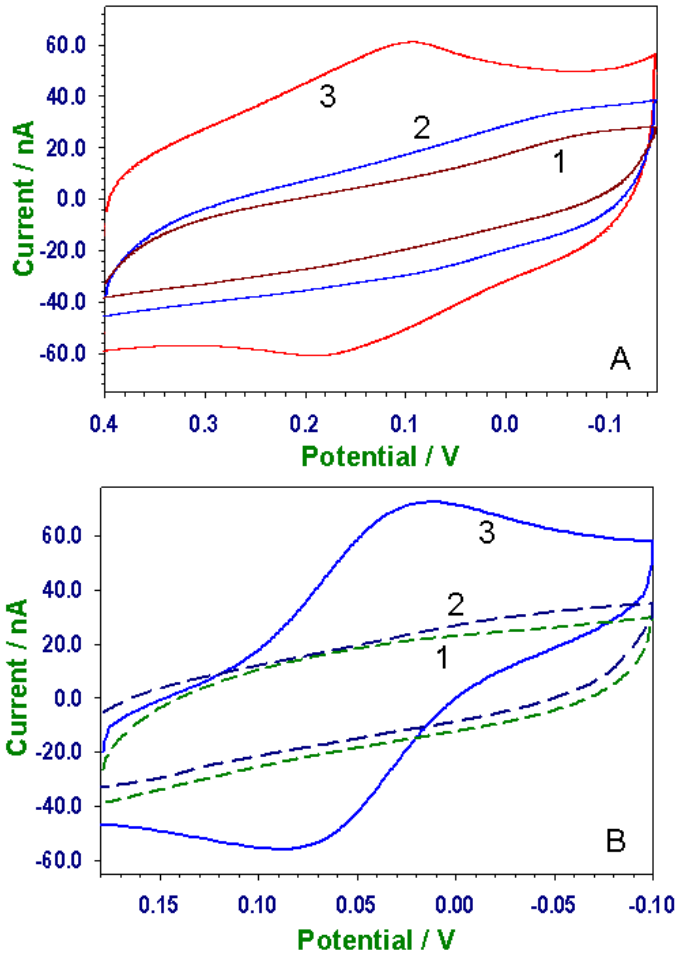

Figure.4. Cyclic voltammogram of HRP coupled to (A) glutathione capped AuNPs, (B) lipoic acid capped AuNPs. Using gold electrode, 10.2 µM H_2O_2, 20 mV/s scan rate, Ag/AgCl reference electrode. Plot (1) is blank electrode, (2) AuNPs modified electrode and (3) is HRP coupled AuNPs modified electrode.

Figure 5 shows the cyclic voltammogram of immobilized HRP-AuNPs at various scan rates. We have observed that there is a linear increase of cathodic and anodic peak current values with the increase of scan rate indicating an electrode process as expected for an immobilized system. The peak potentials shifts very slightly in opposite directions with the change of scan rate, which was similar to other immobilized systems (Ferri et al., 1998, Murray et al., 1984).

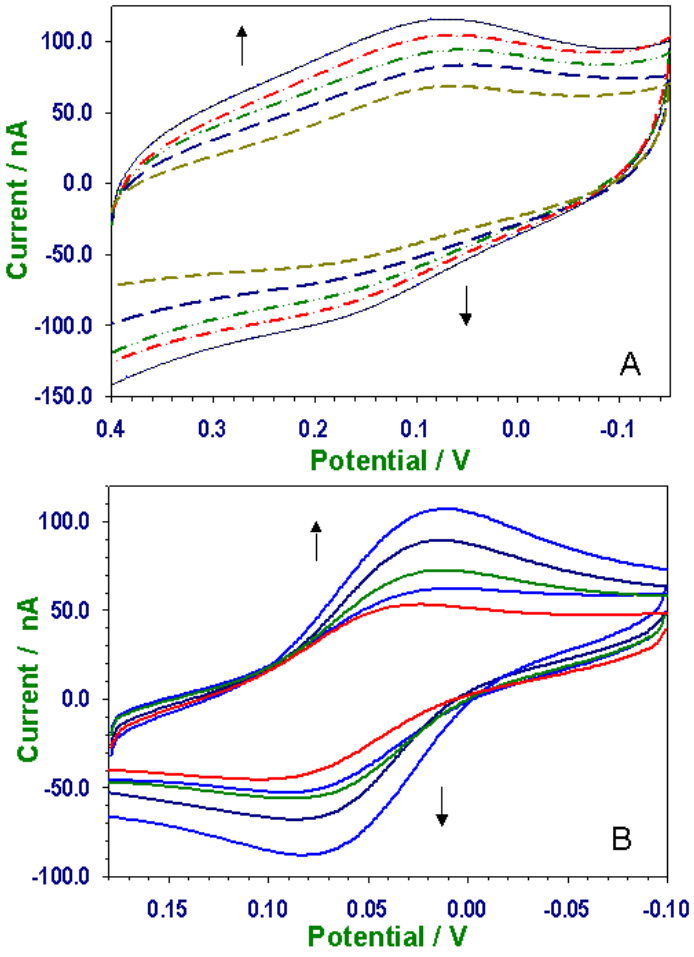

Figure.5. Cyclic voltammogram of HRP coupled to (A) glutathione capped AuNPs, (B) lipoic acid capped AuNPs at scan rates of 5, 10, 20, 40 and 80 mV/s. Using gold electrode, 10.2 µM H_2O_2, Ag/AgCl reference electrode.

3.3.3 Electrochemical studies of HRP-AuNPs electrode using different concentrations of H_2O_2:

The electrochemical studies of HRP-AuNPs conjugate were carried out using different concentrations of H_2O_2 (Figure 6A). There was an increase in the peak current value with the increase in the peroxide concentration and at higher concentration a plateau was obtained. A hyperbolic plot, mimicking Michaelis Menten (MM) kinetics have been fitted to the experimental points for a better visual clarity. The MM plot obtained for both the HRP coupled to glutathione and lipoic acid capped gold nanoparticles matches with the normal plot reasonably well. The optimum concentration for good electrochemical response was observed in the concentrations of 6.8-20.4μM concentration of H_2O_2. At higher concentrations of H_2O_2, we observe the saturation effect, when all the enzyme is present in the oxidized form.

3.3.4 Electrochemical studies of HRP-AuNPs electrode at different pH:

Figure 6B shows the direct electron transfer of immobilized HRP activity at various pH by means of its electrocatalytic behavior to the reduction of H_2O_2. A pH range of 7.2-8.0 was optimal for the good electroactivity of the enzyme. These results were consistent with the known biochemical characteristics of the enzyme. Therefore the observed pH dependence was very similar for both glutathione capped and lipoic acid capped AuNPs and was similar to the pH dependence of the native enzyme (with a small shift of the optimal pH).

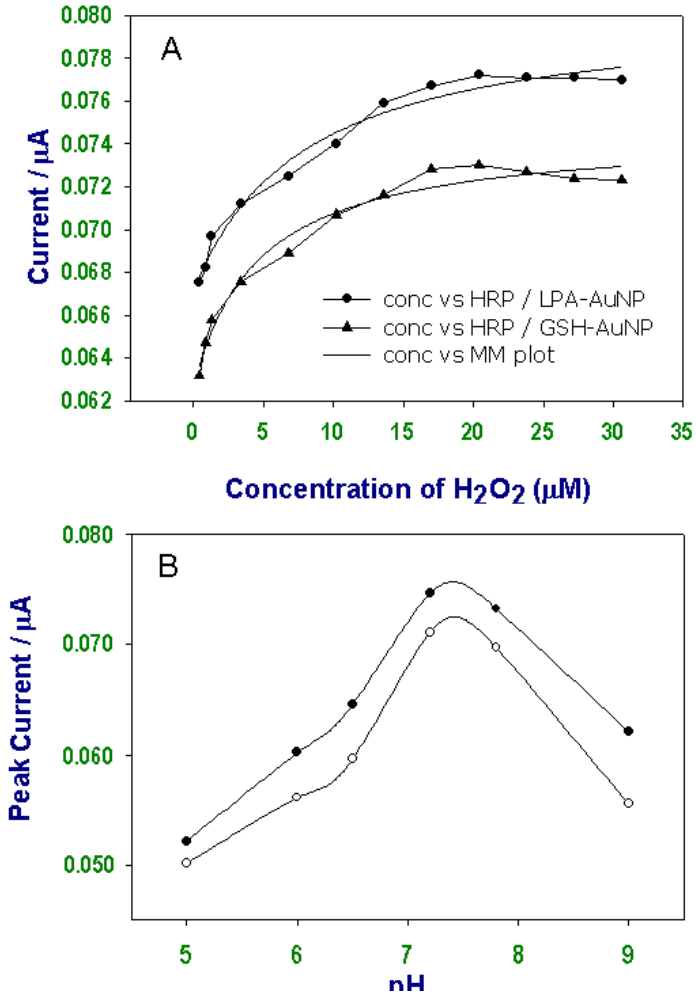

Figure.6. Dependence of the peak current values obtained from cyclic voltammogram of HRP coupled to lipoic acid capped AuNPs (-●-) measured at the potential of 0.06 V and glutathione capped AuNPs (-▲-) measured at a potential 0.01 V using (A) different concentrations of H_2O_2 and at (B) different pH.

3.4 Conclusions

Glutathione and lipoic acid capped gold nanoparticles were prepared by borohydride reduction, which were directly used for covalently attaching the HRP and the resulting AuNPs-HRP bioconjugate was immobilized onto the gold electrode by direct adsorption. The cyclic voltammetry measurement showed good electrochemical response for both HRP coupled to glutathione and lipoic acid capped Au-NP. The peak potential was at E_{pc} = 0.110 V; E_{pa} = 0.182 V and E_{pc} = 0.011 V; E_{pa} = 0.089 V for glutathione and lipoic acid capped gold colloid. Both the glutathione and lipoic acid capped Au-NP modified electrodes showed a good electrochemical response. The optimal activity of HRP labeled AuNPs was between the range pH 7.2-8.0. This study shows that the approach of covalent linking of the enzyme to the nanoparticles needs less time as it forms a more stable attachment (no leaching). Coupled enzyme has full biochemical activity with a spacer arm, which gives a possibility of higher efficiency of electron transport.

A large number of clinical diagnostic tests depends on or uses HRP as a reporter enzyme and uses a color reaction in which a suitable dye is used as an electron acceptor. Conventional ELISA tests depend exclusively on HRP to report the presence of selected antibodies. We propose that the HRP electrode can be successfully used as an electrochemical tool instead of a colorimetric assay, as this mode of operation is faster, more accurate and less prone to noise. The protocol outlined in this experiment can be used for any common

enzyme with very little modifications and therefore offers the possibility of developing arrays of sensors using this covalent coupling technique.

3.5 References

- Berglund, G. I *et al*., (2002). The catalytic pathway of horseradish peroxidase at high resolution. *Nature*, 417, 463-468
- Chance, B. (1957). "Advances in Enzymology", (Eds. F.F. Nord), Vol 12 Intersciences Publishers, 153-190.
- Chance, B. (1951). "The Enzymes", (Eds. J B Sumner and K Myrback), Vol 2, Part 1, Academics Press New York
- Chmielnicka, J., P Ohlsson, P. (1971). *FEBBS Lett*, 17, 181.
- Dawson, J. (1998). Probing structure-function relations in heme-containing oxygenases and peroxidases. *Science*, 240, 433.
- Di, J., Shen, C., Peng, S., Tu, S., Li, S. (2005). A one-step method to construct a third-generation biosensor based on horseradish peroxidase and gold nanoparticles embedded in silica sol–gel network on gold modified electrode. *Anal. Chim. Acta. 553*, 196-200.
- Ferri, T., Pscia, A., Santucci, R. (1998). *Bioelectrochem. Bioenerg*. 44, 177-181; 45, 221-226.
- Gao, F., Yuan, R., Chai, Y., Chen, S., Cao, S., Tang, M. (2005). Amperometric hydrogen peroxidebiosensor based on the immobilization of HRP on nano-Au/Thi/poly (p-aminobenzene sulfonicacid)-modifiedglassy carbon electrode. *J. Biochem. Biophys. Methods*, *70*, 407-413.
- Harbury, H. A, (1957). *J. Biochem*. 2, 1009-1024.

- Joensson, G., (1991).Reagentless hydrogen peroxide and glucose sensors based of peroxidase immobilized on graphite electrode. *Electroanalysis*, *3*, 741-750.
- Jia, J., Wang, J., Wu, A., Cheng, G.; Li, Z., Dong, S., (2002). A Method to Construct a Third-Generation Horseradish Peroxidase Biosensor: Self-Assembling Gold Nanoparticles to Three-DimensionalSol−Gel Network. *Anal. Chem*. 74, 2217-2223.
- Jose, M, P., Paloma, Y,S., Arceli, G,C. (2008). Gold nanoparticles based electrochemical biosensors. *Electrochimica acta*. 53, 5848.
- Liu, S.Q., Ju, H.X. (2002). Renewable reagentless hydrogen peroxide sensor based on direct electron transfer of horseradish peroxidase immobilized on colloidal gold-modified electrode. *Anal.Biochem*., 307, 110-116.
- Liu, Y., Yuan, R., Chai, Y., Tang, D., Dai, Y., Zhong, X. (2006). Direct electrochemistry of horseradish peroxidase immobilized on gold colloid/cysteine/nafion-modified platinum disk electrode. *Sens.Actuat*.. B, 115, 109-115.
- Luo, X.L., Xu, J.J., Zhang, Q., Yang, G.J., Chen, H.Z. (2008). Electrochemically deposited chitosan hydrogel for horseradish peroxidase immobilization through gold nanoparticles self-assembly, *Biosens. Bioelectron*., 21, 190-196. (http://metallo.scripps.edu/PROMISE/PEROXIDASES.html).

- Mehly, A. C, Chance, B. (1954). *Methods Biochem Ana.l*, 1, 357.
- Mehly, A.C. (1952). *Biochem. Biophys. Acta*., 81, 1-17.
- Mehley, A., C. (1995). Plant Peroxidase in "M*ethods of Enzymology*", (Eds. S.P. colowick, N.O. Kaplan), Vol 2, Academic Press, New York 801-813.
- Morrison, M, Bayse, G, (1973). Peroxidase-Catalysed Reactions, Oxidases and Related Redox Systems, (Eds. T. King, H. Mason and >. Morrisson), Univ Pk Press, Baltimore, MD USA, 375.
- Murray, R . W, (1984) in Electroanalytical Chemistry (Bard, J. A., Ed.). Vol. 13. pp. 205. Dekker, New York.
- Razumas, V.J., Gudavicius, A.V., Kulys, J.J. (1983). Redox conversion of peroxidase on surface of 56modified gold electrode. *J. Electroanal Chem*., *151*, 311-315.
- Ruzgas, T., Csoregi, E., Emnéus, J., Gorton, L., Varga, G.M. (1996). Peroxidase-modified electrodes: Fundamentals and application. *Anal Chim Acta*., *330*, 123-138.
- Ruzgas, T., Emnéus, J., Gorton, L., Varga, G.J. (1995). Kinetic models of horseradish peroxidase action on a graphite electrode. *J. Electroanal. Chem*., *391*, 41-49.
- Shannon, M. L., Ekay, J. Y., Lew,(1966), *J. Biochem*., 241, 2166-2172.

- Theorell, H, (1951). The Enzymes, (Eds. J. Summer and K. Myrback), Academic Press, NY, 397.

- Wang, Z., Li, M., Su, P., Zhang, Y., Shen, Y., Han, D., Niu, L. (2008)., Direct electron transfer of horseradish peroxidase and its electrocatalysis based on carbon nanotube/thionine/gold composites. *Electrochem. Commun.,* 10, 306-310.

- Wollenberger, U., Bogdanovskaya, V., Bobsin, S., Scheller, F., Tarasevich, M. (1990). Enzyme electrode using bioelectrocatalytic reduction of Hydrogen peroxide. *Anal. Letts*., *23*, 1795-1797.

- Xiang, C., Zou, Y., Sun, L. X., Xu, F. (2008). Direct Electron Transfer of Horseradish Peroxidase and Its Biosensor Based on Gold Nanoparticles/Chitosan/ITO Modified Electrode. 2008, *Anal. Letts*., 41,2224-2226.

- Yu, Z., Qin, Z.H. (2008). Modified Electrode Based on Immobilizing Horseradish Peroxidase on nano-Gold with Choline Covalently Modified Glassy Carbon Electrode as a Base. *Chin. J .Anal. Chem*., 36, 604-610.

Chapter 4

Gold Nanoparticles Based Sandwich Electrochemical Immunosensor

4.1 Introduction

In the recent years, the field of electrochemical biosensors design has become capable of providing better analytical characteristics in terms of sensitivity, selectivity reliability, ease of use and low cost. Among the various types of electrochemical sensors, immunosensors are the most attractive tools for the detection of analytes based on the binding of antibody and antigens. Unlike other techniques, electrochemical methods are not usually affected by any sample impurities and the instruments required are relatively simple and are of modest cost. Most of the studies in immunosensors concentrate on the electrochemical detection using labeled immunoagent (enzymes are most commonly been used as the labels). The achievement of high sensitivity requires different amplification platforms and processes. It has been shown that, we can enhance the sensitivity of the signal and the detection ability (Storhoff *et al*., 1998; Hu *et al*., 2003; Kumar *et al*., 2008; Parak *et al*., 2003; Tkachenko *et al*., 2003) of the biosensing devices by using nanoparticles in their construction. Use of nanoparticles permits high local concentrations and therefore higher sensitivity. Although different types of nanoparticles have been used earlier for the construction of electrochemical sensors, the use of gold nanoparticles (AuNPs) allows enhanced analytical detection with respect to others.

The ability of AuNP to provide a stable immobilization of biomolecules, in order to retain their bioactivity is a major advantage for the preparation of sensors (as it also has an excellent conducting capability and high surface to

volume ratio). Various approaches like, layer by layer self assembly using nafion (Tang *et al*., 2004), dithiothreitol (Chatrathi *et al*., 2007), cysteamine (Wang *et al*., 2004), 4-aminothiophenol (Wang *et al*., 2004), and polyvinyl butryal (Tang *et al*., 2004) have been used earlier for the construction of immunosensors. In the recent years construction of immunosensors using AuNPs have received significant attention. Besides this antibody was also used in sol-gel matrix (Wu *et al*., 2005) and carbon paste electrode (Dana *et al*., 2007) immunosensors. Some of the earlier works have demonstrated the direct assembly of antibody (Chen *et al*., 2007) and antigen onto the electrode. Taking an account of the advantages and methods used for gold nanoparticles modified electrode preparation, we have prepared gold nanoparticles modified electrode surface by the direct covalent linking of the antibody to the nanoparticles and assembling them onto the electrode surface. In the current study, we have shown that direct linking of antibody to the AuNPs using covalent methods can be used for the development of immunosensors. This kind of approach provides a right orientation of the antibody with the free antigen binding sites available for further immunoreaction without affecting the structure and function of the antibody. The AuNP also helps in the better immobilization of the molecules onto the electrode preventing them from beingdissolved back into the bulk solution.

HRP has been used for the detection purpose in this study because of its small size and high stability to the chemical modifications. Peroxidases are enzymes of the class **EC 1.11.1.7**, which are defined as oxidoreductases that use hydrogen peroxides as electron acceptor. The reaction mechanism for the

enzyme catalytic cycle of HRP (Ruzgas *et al*., 1996) is given below (Scheme 1).

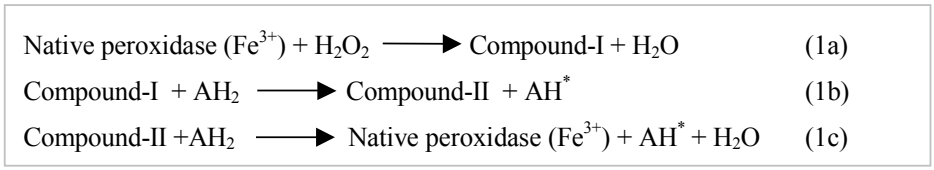

Scheme 1. The reactions in the enzyme catalytic cycle of HRP

The first reaction (la) involves the two-electron oxidation of the ferriheme prosthetic group of the native peroxidase by H_2O_2 (or organic hydroperoxides). This reaction results in the formation of an intermediate, compound-I (oxidation state +5), consisting of oxyferryl iron (Fe (IV) O=0) and a porphyrin π cation radical. In the next reaction (1b), compound-I loses one oxidizing equivalent upon one-electron reduction by the first electron donor AH_2 and forms the compound-II (oxidation state +4). The later in turn accepts an additional electron from the second donor molecule AH_2 in the third step (lc), whereby the enzyme is returned to its native resting state, ferriperoxidase.

3,3', 5,5'-tertramethyl benzidine or TMB is a chromogenic substrate used in the staining procedure of immunohistochemistry and also as a visualizing agent in ELISA. In solution, TMB forms a blue product when allowed to react with peroxidase in the presence of H_2O_2 (Figure 1). The resulting color change can be read at 370 or 655 nm. The reaction is stopped using acid and the color changes to yellow, which it is read at 450 nm.

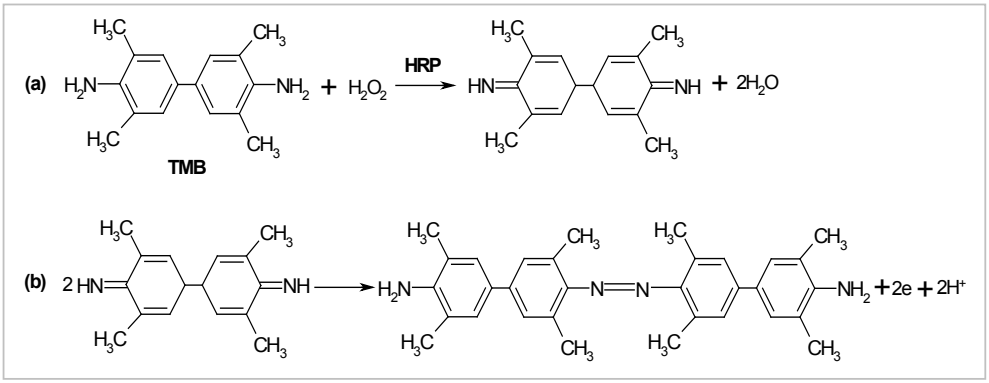

Figure 1. Mechanism of TMB during the (a) enzymatic, where TMB is oxidized during the enzymatic degradation of H_2O_2 by horseradish peroxidase and (b) during the electrochemical reaction the TMB undergoes two-electron oxidation reaction to form an azo product.

4.1.1 Overview of ELISA:

Enzyme-linked immunosorbent assay (ELISA) is a plate-based assay designed for detecting and quantifying substances such as peptides, proteins, antibodies and hormones. Other names, such as enzyme immunoassay (EIA), are also used to describe the same technology. In an ELISA, an antigen must be immobilized onto a solid surface and then complexed with an antibody that is linked to an enzyme. Detection is accomplished by assessing the conjugated enzyme activity via incubation with a substrate to produce a measurable product. The most crucial element of the detection strategy is a highly specific antibody-antigen interaction.

4.1.1.1 Introduction:

ELISA is typically performed in 96-well (or 384-well) polystyrene plates, which will passively absorb antibodies and proteins in a nonspecific manner. It is this binding and immobilization of reagents that makes ELISA so easy to design and perform. Having the reactants of the ELISA immobilized

on to the microplate surface makes it easy to separate bound material from nonbound material during the assay. This ability to wash away nonspecifically bound materials makes the ELISA a powerful tool for measuring specific analytes within a crude preparation.

A detection enzyme or other tag can be linked directly to the primary antibody or introduced through a secondary antibody that recognizes the primary antibody. It also can be linked to a protein such as streptavidin if the primary antibody is biotin labeled. The most commonly used enzyme labels are horseradish peroxidase (HRP) and alkaline phosphatase (AP). Other enzymes have been used as well, but they have not gained widespread acceptance because of their limited substrate options. These include β-galactosidase, acetylcholinesterase and catalase. A large selection of substrates is available for performing the ELISA with an HRP or AP conjugate. The choice of substrates depends upon the required assay sensitivity and the instrumentation available for signal-detection (spectrophotometer, fluorometer or luminometer).

4.1.1.2 ELISA Formats:

ELISA can be performed with a number of modifications to the basic procedure. The key step, immobilization of the antigen of interest, can be accomplished by direct adsorption to the assay plate or indirectly via a capture antibody that has been attached to the plate. The antigen is then detected either directly (labeled primary antibody) or indirectly (labeled secondary antibody). The most powerful ELISA assay format is the sandwich assay. This type of

capture assay is called a "sandwich" assay because the analyte to be measured is bound between two primary antibodies – the capture antibody and the detection antibody. The sandwich format is used because it is sensitive and robust (Figure 2).

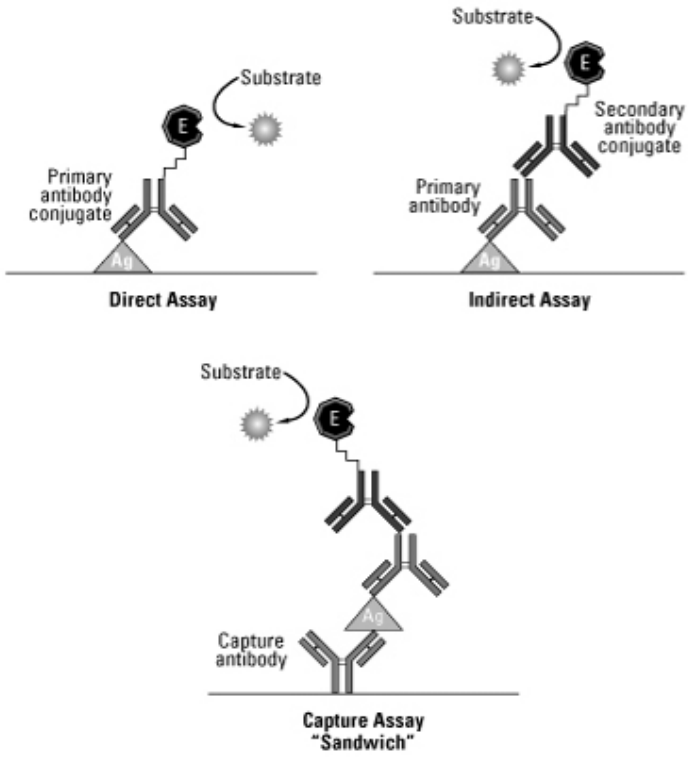

Figure 2. Common ELISA formats. In the assay, the antigen of interested is be immobilized by direct adsorption to the assay plate or by first attaching a capture antibody to the plate surface. Detection of the antigen can then be performed using an enzyme-conjugated primary antibody (direct detection) or a matched set of unlabeled primary antibody and conjugated secondary antibodies (indirect detection) and capture or primary antibody used to capture the antigen in sandwich method.

4.2 Materials and methods

4.2.1 Materials and instrumentation:

For the present study, we have used anti-human serum albumin (HSA) (Ab_1), HSA (Ag) and HRP labeled antibody (Ab_2) from Bangalore Genei (India) and *N*-Ethyl-*N*′-(3-dimethylaminopropyl) carbodiimide hydrochloride (EDC) was purchased from Sigma. Gold chloride [$AuCl_4$, $4H_2O$, Au% > 49%] and all other chemicals were of the analytical grade and were used without further purification. All the solutions were prepared using double distilled water.

The absorption spectrum of the samples was recorded in UV-1601 PC (Shimadzu). Electrochemical measurements were performed using CH Instruments 660A with three electrode system, comprising of platinum auxiliary electrode, an Ag/AgCl reference electrode and a gold electrode (as the working electrode). The 1:1 ratio of 0.1M phosphate buffer (PB) pH 7.4 and 0.1M KCl was used as electrolyte for all the measurements.

4.2.2 Methodology:

4.2.2.1 Synthesis of sodium borohydride reduced gold nanoparticles:

All the glassware used for the preparation were cleaned and soaked in freshly prepared HNO_3/HCl mixture, and then they were rinsed thoroughly in distilled water and dried in air. In a typical preparation of gold nanoparticles a quantity of 100 ml of 330 μM concentrated aqueous solution of choloroauric acid ($HAuCl_4$) was reduced by 400 μl of freshly prepared 66 mM sodium

borohydride ($NaBH_4$) aqueous solution under room temperature by adding dropwise with stirring to yield ruby red solution of gold nanoparticles. The solution was subjected to ultracentrifugation and the resulting pellet was washed with double distilled water twice. The pellet was than redispersed in water for UV-VIS spectroscopy studies and TEM analysis. For FTIR analysis the pellet was dried and the powder was used for sample preparation.

4.2.2.2 Preparation of glutathione capped AuNPs:

To the gold colloid solution prepared as stated above, the capping was done by the addition of 1 ml of 65 mM of glutathione to 100 ml of gold solution and the mixture was stirred for 10-15 minutes. After the addition of glutathione and aging of gold nanoparticles solution for 2 h, the solution was subjected to centrifugation and the resulting pellet obtained was washed twice with double distilled water to remove unbound glutathione residues. The pellet was than redispersed in water for UV-VIS spectroscopy studies and TEM analysis. For FTIR analysis the pellet was used for sample preparation.

4.2.2.3 Preparation of AuNP-Antibody conjugate:

AuNP-Antibody was prepared in two steps:

(i) Covalent linking of 1,6 diamino hexane (DAH) to AuNPs:

In the first step the carboxylic groups present in the glutathione and lipoic acid was activated by EDC. The capped AuNP (0.5 mg) were dissolved in pH 5.0 MES buffer (3 mL) and 58 mM EDC (300 µL) was added and the reaction mixture was kept at 4^oC for 1.5 h on a rocker. After the reaction time the solution was centrifuged at 15,000 rpm for 1 h to separate carbodiimide

activated AuNPs. To the pellet 50 µL of 500 µM 1,6-diaminohexane (DAH) in 0.1 M phosphate buffer was added to the activated AuNPs and mixed for 30 minutes at room temperature and the reaction mixture was again centrifuged and the pellet obtained was washed twice with distilled water to separate unbound DAH and the AuNP-DAH was redissovled in 0.1 M phosphate buffer.

(ii) Covalent linking of antibody to AuNP-DAH:

In the next step 500 µL of 10 µg/mL primary antibody was added to pH 5.0 MES buffer (3 mL), to that 58 mM EDC (300 µL) was added and the reaction mixture was kept at 4^oC for 1.5 hrs on a rocker. The activated primary antibody was added to AuNP-DAH and the reaction mixture was kept at 4^oC for 6 h. After the reaction time the coupled AuNP-Antibody$_1$ (AuNP/Ab$_1$) conjugate was separated by centrifugation (Scheme 2).

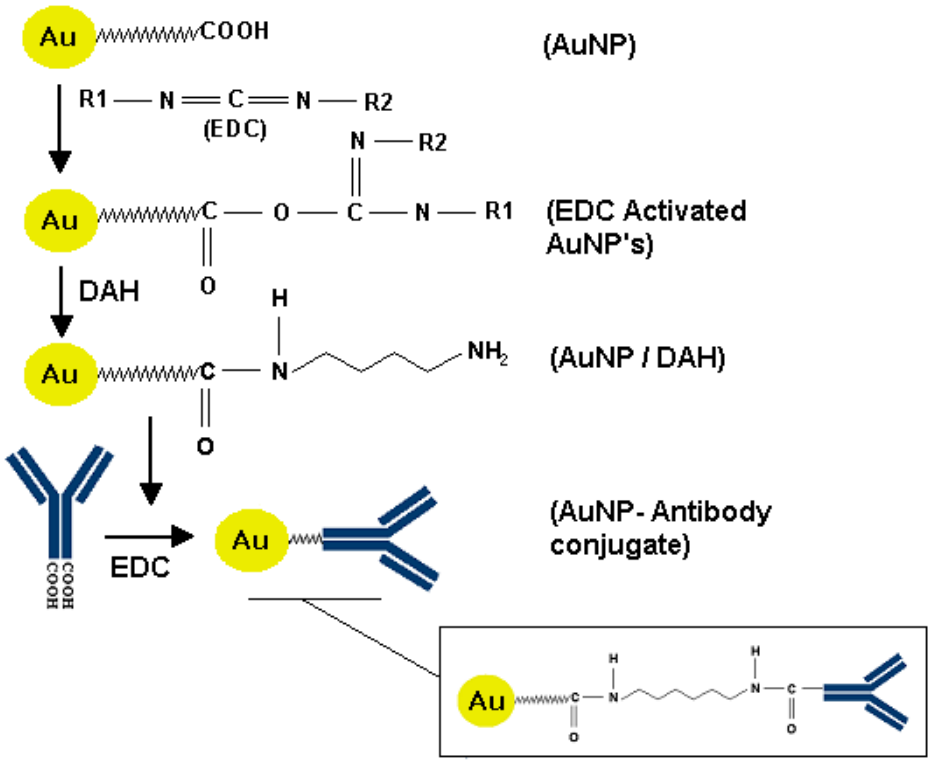

Scheme 2. Schematic representation of the preparation of AuNP/Ab_1 conjugate involving two steps (1) Covalent linking of DAH to the carbodiimide activated AuNP, (2) Attaching carbodiimide activated antibody to the AuNP-DAH.

4.2.3 Antibody immobilization and immunoassay procedure:

AuNP/Ab_1 was immobilized onto the gold electrode. 5 µL of AuNP/Ab_1 solution was spread onto the cleaned and polished gold electrode and the electrode was incubated at 4^oC. After the incubation, the electrode was rinsed and then the electrode was blocked with 1% BSA + 0.05% tween for 30 mins at room temperature. The electrode was rinsed again to remove any residuals. The AUNP/Ab_1 electrode was then incubated with a 5 µL of antigen for 30 mins at room temperature. After the binding of antigen, the electrode was incubated in 50 µL of 2 mg/ml Ab_2/HRP conjugate. Finally the electrode was washed to remove unbound conjugate. Scheme 3 shows the schematic representation of the immobilization procedure.

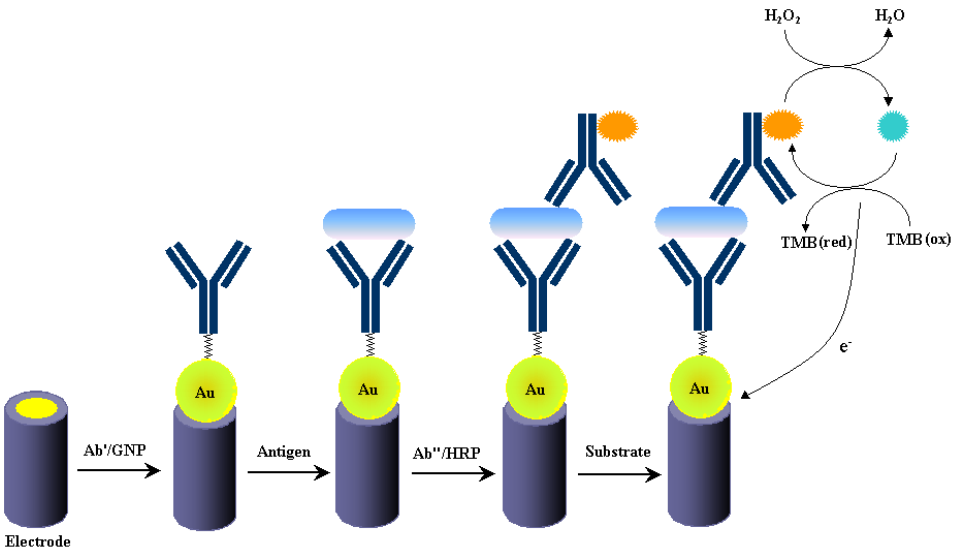

Scheme 3. Schematic representation of the immunoassay step done onto the gold electrode.

4.2.4 Measurement procedure:

The modified electrode was then placed in electrochemical cell containing 2.0 ml of 0.1 M PB (pH 7.4) and 0.1 M KCl. TMB (15μM) was used as electron mediator and H_2O_2 (20 μM) was used as substrate. The cyclic voltammetry measurements were done at the potential range of 450 to – 300 mV at a scan rate of 10mV/s and Ag/AgCl as the reference electrode. The impedance measurements were done at the frequency range of 0.1 to 1.0×10^{-5} Hz at room temperature (Z_{re} Vs. Z_{im} at 160 mV vs. Ag/AgCl reference electrode).All the electrochemical measurements were performed at room temperature.

4.3 Results and Discussions

4.3.1 UV-Visible spectroscopy studies:

The gold nanoparticles synthesized by borohydride reduction of aurate salt are relatively monodisperse in colloidal solution, which is confirmed by a single peak in the absorbance spectra (Figure 3a) . The λ_{max} was observed at around 530 nm. In the next step, which involved the protection of nanoparticles for stability, we have used glutathione as the capping or protecting agent. As shown in the Figure 3b, the peak is shifted towards the higher wavelength after capping with glutathione. The λmax was observed at around 540-580 nm and the change of color was also seen from wine red to blue color after capping.

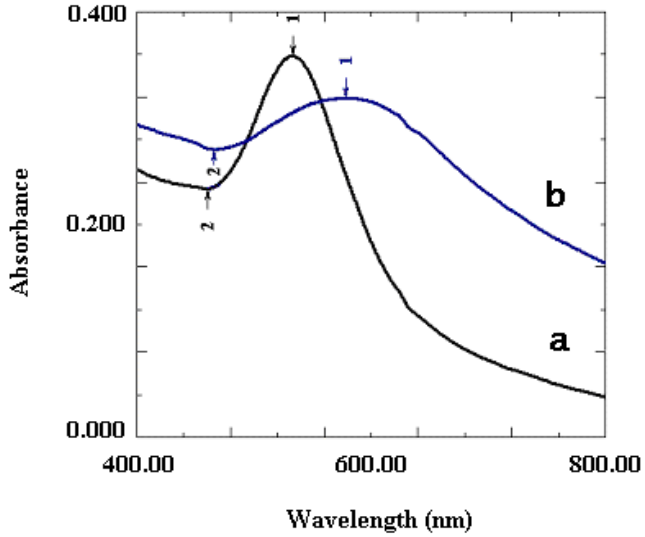

Figure 3. UV-Visible spectrum of (a) gold nanoparticles (AuNP), (b) glutathione capped AuNPs.

4.3.2 Electrochemical studies:

HRP catalyzes the reaction; in which reduced TMB is oxidized in the presence of H_2O_2.

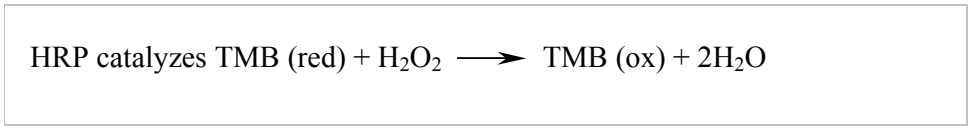

The enzyme activity can be measured by the voltammetric detection of the reduction current generated by TMB at the gold electrode. Electrochemical investigation of the TMB and the modified electrode was carried out using gold electrode. The most interesting results in terms of the generated electrocatalytic current were observed with TMB in the presence of the enzyme. This is given in the Figure 1, which shows the enzymatic and electrochemical reaction mechanism of TMB.

4.3.2.1 Cyclic voltammetry of the immunosensors:

The cyclic voltammetry of the (AuNP-Ab_1)(Ag)(Ab_2-HRP) modified gold electrode (MGE) was done in PB/KCl at a scan rate of 10 mV/s and sweeping range of 450 mV to –300 mV (Figure 4A). The results in the Figure 4A(1) show no change in response with the presence of only H_2O_2 in the solution. Where as the CV of only TMB in the solution using the modified electrode, showed two peaks at the potential 240 mV and -35 mV [Figure 4A(2)]. The voltammogram in the presence of both H_2O_2 and TMB [Figure 4A(3)] showed two well-defined new peaks at the potential 154 and –156 mV. The current value of the peak at -33 mV was increased. The new peaks developed were due to the further electrochemical oxidation of oxidized TMB

(Figure 1) When compared to CV without adding H_2O_2, the CV of TMB showed two peaks at 240 mV and 35 mV, which was due to the electrochemical oxidation of TMB.

Figure 4B shows the voltammogram of various blanks at various stages of modification of the gold electrode using 15 μM TMB/ 20 μM H_2O_2 in 0.1M PB/KCl at potential range of 450 mV to –300 mV and 10 mV/s scan rate. There were no peaks for the blank gold electrode, AuNP-Ab_1, and AuNP-Ab_1/Ag. But when secondary antibody HRP conjugate was added to the AuNP-Ab_1/Ag electrode, the voltammogram showed two well defined peaks. In voltammogram, the redox peaks at potential 154 mV, -33 mV and -0.156 mV corresponds to the oxidized TMB.

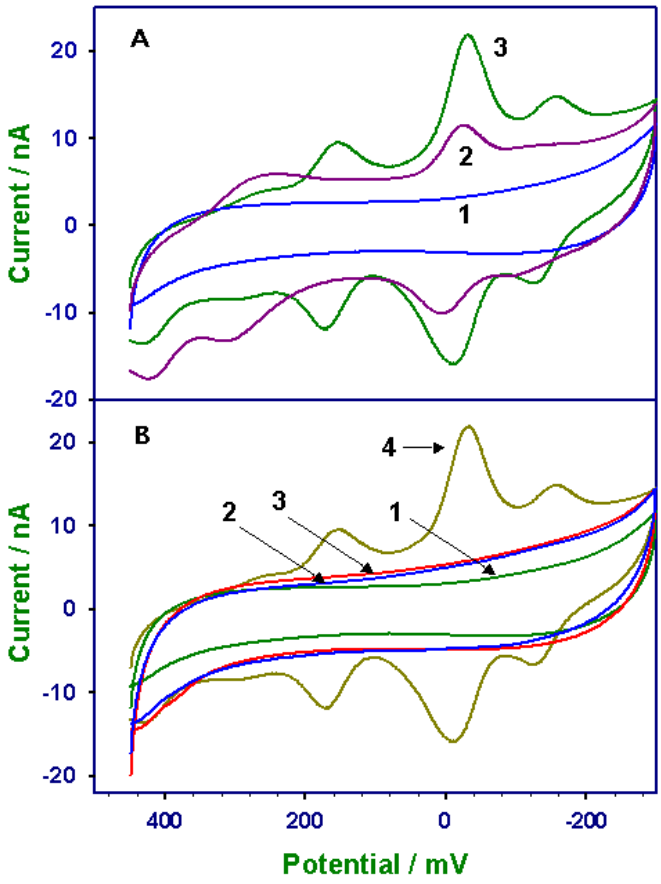

Figure 4. (A) Voltammogram of modified electrode (1) only 20 µM H_2O_2, (2) only 15 µM TMB, and (3) 15 µM TMB + 20 µM H_2O_2 and **(B)** Voltammogram of (1) blank gold electrode, after stepwise immobilization of (2) primary antibody, (3) antigen and (4) HRP coupled secondary antibody. In 0.1 M PB (pH 7.4) at a potential range of 450 mV to -300 mV, vs. Ag/AgCl reference electrode. Scan rate 10 mV/s.

4.3.2.2 Study of the immunosensors using different antigen concentrations:

The electrochemical study was done using different concentrations of antigen to check the sensitivity of the modified electrode. The antigen concentrations used were 2, 4, 8, 16, 32 ng/ml. 5 µl each of the analyte was immobilized onto the electrode and the electrochemical measurements were done. Figure 5 shows that, upto 2 ng/ml sample, which equals to 10 pg/5 µL of the antigen was easily detected and showed a defined CV.

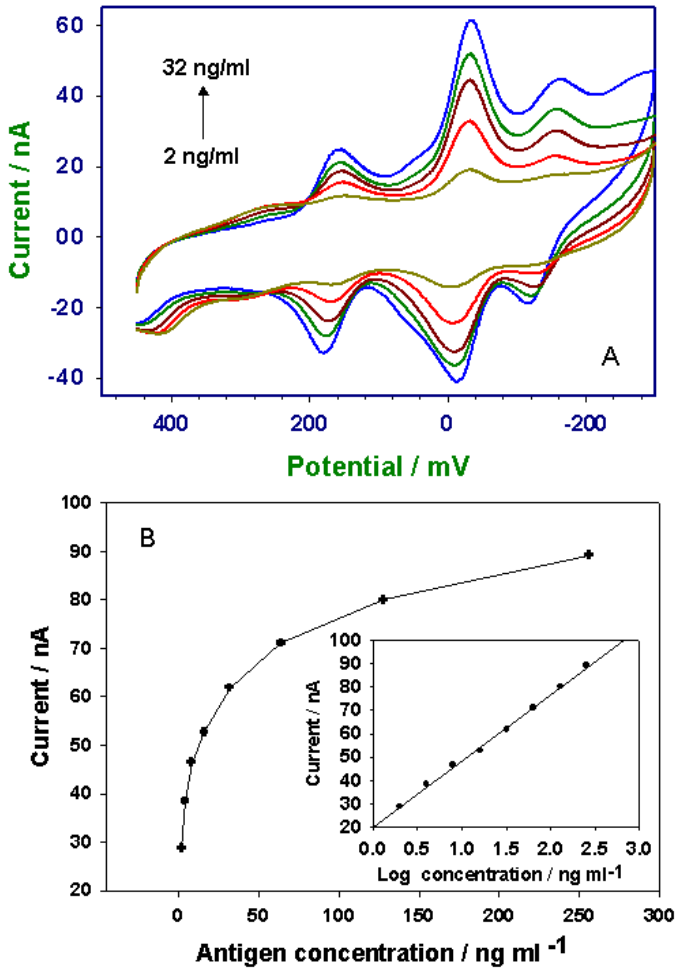

Figure 5. (A) Voltammogram of modified electrode using different concentrations of antigen in 0.1 M PB/0.1 M KCl (pH 7.4) at a potential range of 450 mV to -300 mV, vs. Ag/AgCl reference electrode. Scan rate 10 mV/s (B) Plot showing the dependence of peak current values of cyclic voltammogram done using different concentrations of antigen. Inset is log plot.

4.3.2.3 Optimization of immunoassay condition:

The factors like concentrations of primary antibody (Ab_1), HRP conjugated secondary antibody (Ab_2), pH of incubation solution and incubation time was studied. The effect of the concentration of Ab_1 and Ab_2 (Figure 6a) were studied using different concentrations of the antibody solution respectively. We have noted that for both the Ab_1 and Ab_2, as the concentration of antibodies was increased there was an increased in the peak current value, which showed that the AuNPs facilitated the electron transport between the HRP/dye and the electrode. But after the concentration of more than 2 μg/mL for Ab_1 and 5 μg/mL for Ab_2 the response reached a constant value indicating that the amount of the Ab_2 wase enough to match the amount of Ab_1 molecules existing on the surface of the electrode.

Other factors that influenced the immunoreaction included pH of the incubation solution and the incubation time. The optimal pH range was between the pH 7.2 and 7.8, with good response seen at pH 7.4 (Figure 6b).

The response of electrode with increasing incubation time of antigen was studied upto 60 minutes (Figure 6c). The response showed that the longer incubation time did not enhance the response with optimal incubation time of 20-25 minutes.

Therefore the optimal conditions for good response of the electrode was 2 μg/mL Ab_1, 5 μg/mL Ab_2 in 2 mL of 0.1 M PB 0.1 M KCl of room temperature with 20 minutes for good antigen-antibody interaction time.

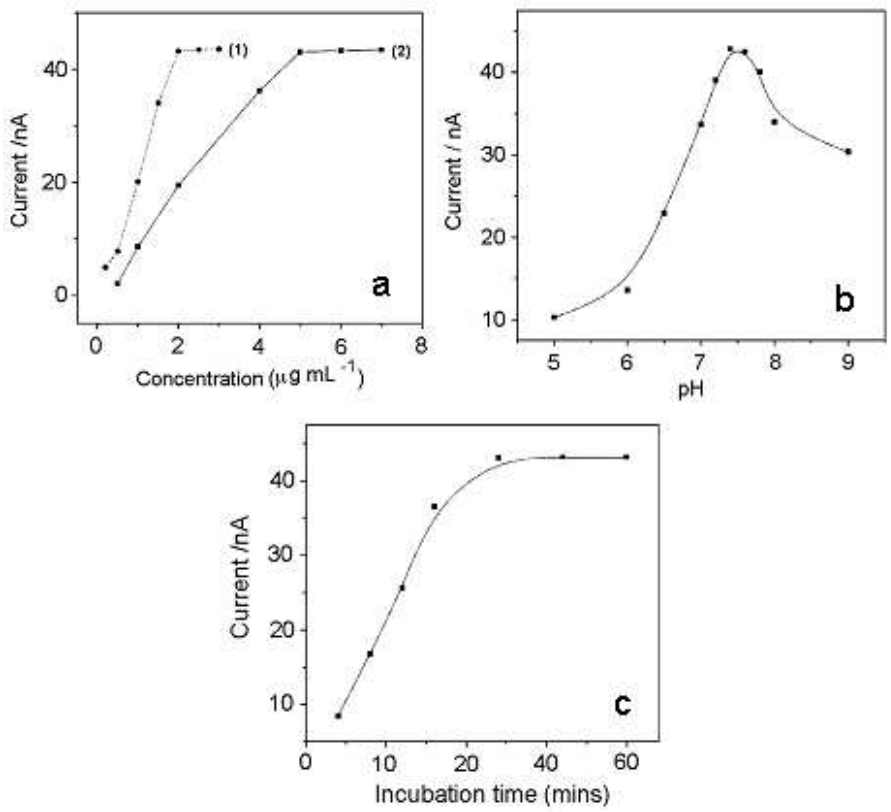

Figure 6. Effects of (a) concentrations of primary Ab (1) and HRP conjugated secondary antibody (2), (b) pH of incubation solution, (c) incubation time, and when one condition is changed, other conditions are pH 7.4, 5 μg/mL Ab_1, 2 μg/mL HRP-Ab_2 and 20 minutes.

4.3.2.4 Identification of the peaks:

As shown in the Figure 2, the cyclic voltammogram of the TMB in the presence of H_2O_2 showed three well-defined peaks. Two sets of experiments were performed to confirm that the peaks observed are due to the oxidation of TMB.

First set: Using low dye concentration, the cyclic voltammetry was done using two different concentrations of H_2O_2 and different scan rates. One experiment was performed using 1 μM of TMB concentration in the solution and the H_2O_2 concentration was 10 μM and 100 μM using the modified gold electrode at the potential range of 450 mV to -300 mV and 10 mV/s scan rate (Figure 7A). The other experiment was done at different scan rates of 10, 30, 50, 100 mV/s (Figure 7B).

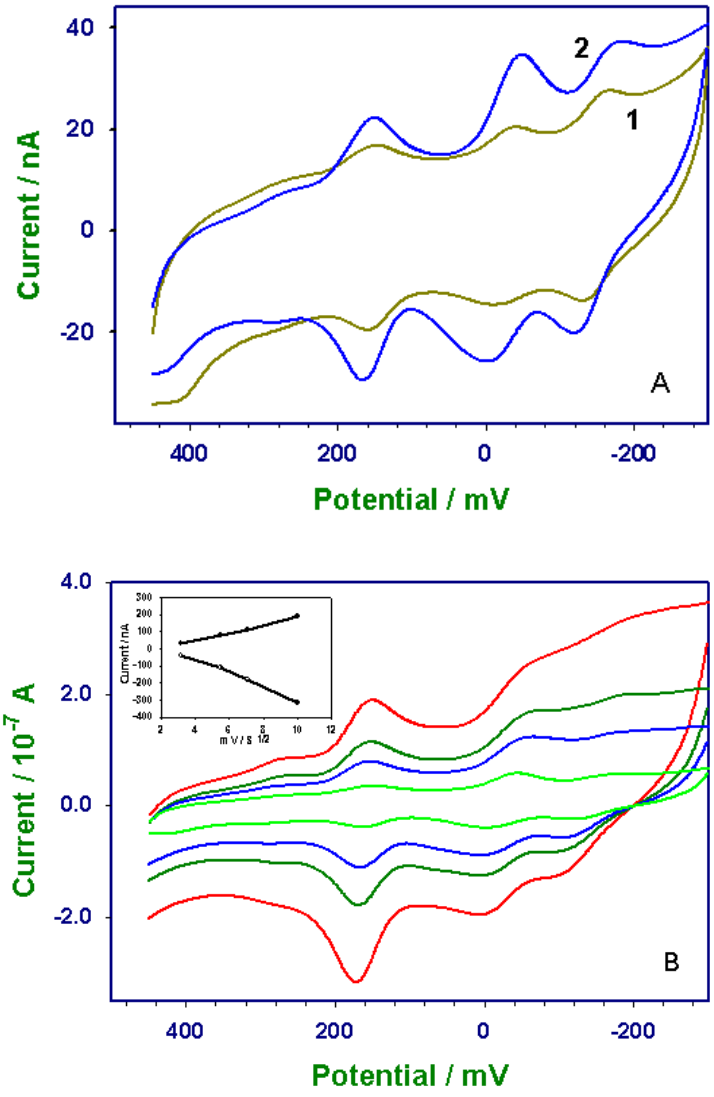

Figure.7. (A) Cyclic voltammogram of (1) 2.5 µM and (2) 25 µM TMB in 0.1 M PB/ 0.1 M KCl (pH 7.4) at a potential range of 450 mV to -300 mV, vs. Ag/AgCl reference electrode. Scan rate 10 mV/s. (B) Voltammogram of 1 µM TMB at a scan rate of 10, 30, 50, 100 mV/sec.

Second set: In this set of experiments, we have used low concentration of H_2O_2, the cyclic voltammetry was done at two different concentrations of the dye and two different scan rates. The experiment was performed using 5 μM of H_2O_2 in the solution and 2.5 μM and 25 μM of TMB using the modified gold electrode at the potential range of 450 mV to –300 mV and 10 mV/s scan rate (Figure 8A). The other experiment was done at different scan rates of 10, 30, 50, 100 mV/s (Figure 8B).

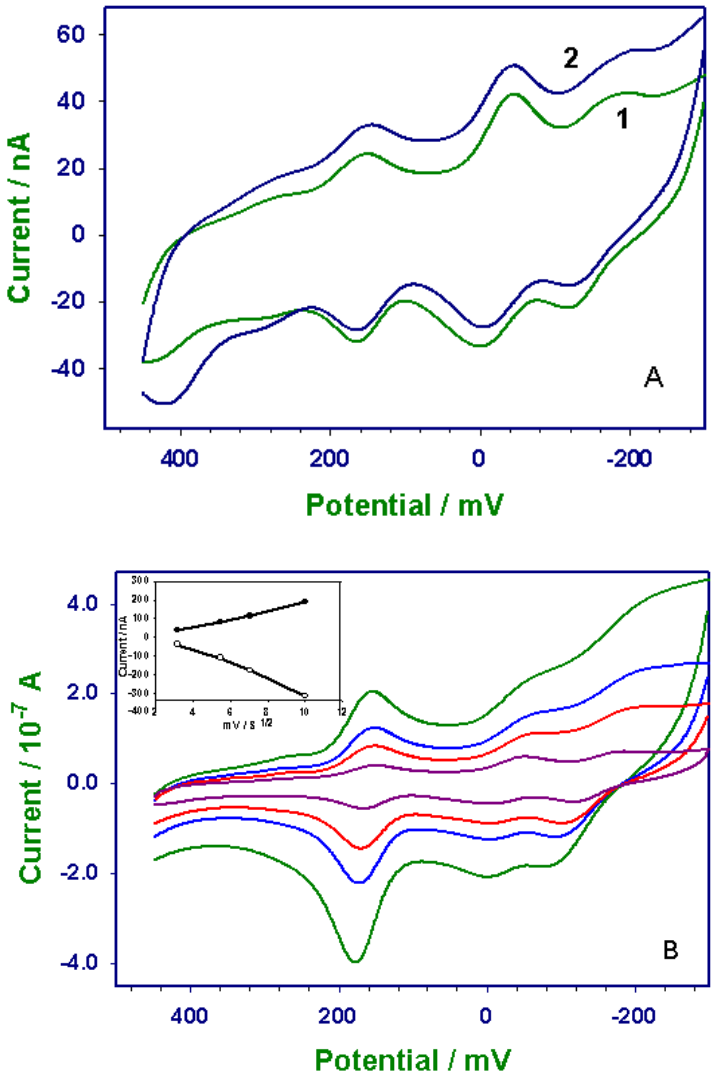

Figure.8. (A) Cyclic voltammogram of (1) 10 mM and (2) 100 mM H_2O_2 in 0.1 M PB/ 0.1 M KCl (pH 7.4) at a potential range of 450 mV to -300 mV, vs. Ag/AgCl reference electrode. Scan rate 10 mV/s. (B) Voltammogram of 1 μM TMB at a scan rate of 10, 30, 50, 100 mV/sec.

If the potential difference ($E_{pc} - E_{pa}$) is ~57 mV, we can say that it is a single electron transfer with the diffusion of the redox species, but if it is ~28 mV than the process is two electron transfer and the redox species is in the solution. To check this we have calculated the potential differences from the CV (Figure 7A and 8A) and represented it in the table below. The potential difference of both the voltammogram, using different concentrations of the dye and H_2O_2 shows that the peak at 154 mV (Figure 7A and 8A) is a two electron process (which represents the reaction 1(a)), and the peak at –33 mV (Figure 7A and 8B) and peak at –156 mV (Figure 7A and 8A) (which represents the scheme 1(b) and 1(c)), are one electron process.

The CV at different scan rates for both 1 μM of TMB and 5 μM of H_2O_2 showed a linear increase in the peak current values with increasing scan rates.

Table 1. (a) Potential difference values calculated from the CV of different concentrations and (b) Peak current difference values calculated from the CV of different scan rate of dye and hydrogen peroxide.

(a)	**[TMB]**	*ΔPeak 1*	*ΔPeak 2*	*ΔPeak 3*	**[H_2O_2]**	*ΔPeak 1*	*ΔPeak 2*	*ΔPeak 3*
	2.5 μM	3 mV	51 mV	31 mV	10 μM	20 mV	49 mV	76 mV
	25 μM	15 mV	50 mV	65 mV	100 μM	13 mV	50 mV	72 mV
(b)	(Ip100 mV/s)/(Ip10 mV/s)				(Ip100 mV/s)/(Ip10 mV/s)			
	[TMB]	*Peak 1*	*Peak 2*	*Peak 3*	**[H_2O_2]**	*Peak 1*	*Peak 2*	*Peak 3*
	1 μM Cathodic	2.8	2.7	3.1	**5 μM Cathodic**	2.5	2.2	2.4
	1 μM Anodic	2.8	2.2	2.8	**5 μM Anodic**	2.7	2.1	2.8

$\Delta Peak = E_{pc}\ E_{pa}$

To show that the dye and H_2O_2 are in the solution and the rate is diffusion controlled, we have calculated the ratio of TMB and H_2O_2 peak cathodic current values for the 100 and 10 mV/s scan rates as shown in Table 1 above. The value should be near unity as shown in the equation below.

$$\frac{I_{peak}}{(\text{scan rate})^{1/2}} = 1$$

Where $(\text{scan rate})^{1/2}$ is the ratio of scan rates 100/10 mV/s = 3.16

And I_{peak} is the ratio of Ipc_{100}/Ipc_{10} and Ipa_{100}/Ipa_{10}

Or $I_{peak} = 3.16$

The above values in the Table 1 are nearly equal to 3.16, which shows that the substrates are in the solution and the electron transfer is diffusion controlled.

4.3.3 Electrochemical impedance spectroscopy (EIS) studies:

EIS is an effective method to monitor the changes of the surface modified electrodes allowing the understanding of the chemical transformation and processes associated with the conductive electrode (Bard and Faulkner 2001). The impedance spectra include a semicircle portion and a linear portion. The semicircle portion at higher frequencies corresponds to the electron transfer limited process and the linear part at lower frequencies corresponds to the diffusion process. The semicircle also corresponds to the electron transfer resistance. Figure 9 exhibits the Nyquist plot of the impedance spectroscopy of the bare and modified electrodes. In EIS, the bare electrode exhibited an almost straight line (Figure 9a), the Nyquist plot (Figure 9b) of glutathione coated AuNPs showed a much lower resistance, implying that the AuNPs are acting as good electron conducting materials and there was also electron transfer between the redox probe and the electrode. When compared to the other electrodes the semicircle diameter was increasing with the addition of the AuNP-Ab_1 (Figure 9c), AuNP-Ab_1/Ag (Figure 9d) and AuNP-Ab_1/Ag/Ab_2 (Figure 9e), suggesting that the series of additions blocked the electron transfer between the redox probe and the electrode. The above results clearly confirm the success of the assembly on the electrode.

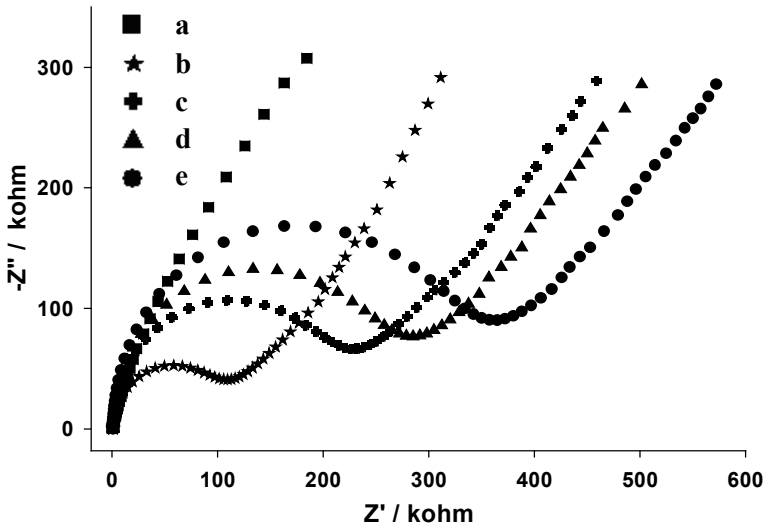

Figure 9. EIS of (a) bare gold electrode, (b) glutathione coated gold nanoparticles, (c) AuNP-Ab conjugate, (d) AuNP-Ab/Antigen, (e) AuNP-Ab/Antigen/Antibody-HRP modified gold electrode in the background solution of TMB and PB/KCl (0.1M, pH 7.4). The frequency range used was 0.1 to 1.0×10^{-5} Hz at room temperature (Z_{re} vs. Z_{im} at 160 mV vs. Ag/AgCl). The series resistance is seen to increase from 100 k to about 350 k as the electrode is successively modified.

4.4 Conclusions

Many different methods have been reported widely for the preparation of electrochemical immunosensors. This study shows the direct linking of antibody to AuNPs using a spacer arm. It not only provides the right orientation of the antibody to bind with the antigen but also the AuNPs used has good conducting capabilities to pass the electron to the electrode for the detection. This electrode provides a novel means for the antibody immobilization and antibody-antigen interaction studies. The cyclic voltammetry measurements were done using TMB that had shown a couple of clear and well defined peaks and the detection limit was found to be 2 ng/ml or 10 pg/5µl of the sample. The impedance measurements showed the formation of the antibody-antigen interaction. We suggest that the sensitivity of the sensors is good but can be increased using flow injection system. We propose that this kind of approach is simple, faster and cost effective and can be used for developing an immunosensor.

4.5 References

- Bard, A.J., Faulkner, L.R. (2001). Electrochemical Methods: Fundamentals and Applications. Third ed. Wiley, New York.
- Chatrathi, M.P., Wang, J., Collins, G.E. (2007). Sandwich electrochemical immunoassay for the detection of Staphylococcal enterotoxin B based on immobilized thiolated antibodies, *Biosens and bioelectron.,* 22, 2932-2938.
- Chen, H., Jiang, J.H., Huang, Y., Deng, T., Li, J. S., Shen, G. L.; Yu, R. Q. (2007). An electrochemical impedance immunosensor with signal amplification based on Au-colloid labeled antibody complex, *Sensors and Actuators B*., 117, 211–218.
- Dana, D.; Xiaoxing , X., Wang, S., Aidong,Z. (2007). Reagentless amperometric carbohydrate antigen 19-9 immunosensor based on direct electrochemistry of immobilized horseradish peroxidase, *Talanta*, 71, 1257-1267.
- Hu, S.Q., Xie, J.W., Xu, Q.H., Rong, K.T., Shen, G.L., Yu, R.Q. (2003). A label-free electrochemical immunosensor based on gold nanoparticles for detection of paraoxon, *Talanta, 61*, 769-777.
- Kumar, S., Aaron, J., Sokolov. (2008). Directional conjugation of antibodies to nanoparticles for synthesis of multiplexed optical contrast agents with both delivery and targeting moieties, *Nat.Protoc., 3*, 314-320.

- Parak, W.J., Gerion, D., Pellegrino, T., Zanchet, D., Micheel, C., Williams, S.C., Boudreau, R., Gros, M.AL., Larabell, C.A., Alivisatos. (2003). Biological applications of colloidal nanocrystals, *Nanotechnology*, *14*, R15–R27.

- Ruzgas, T., Csoregi, E., Emnéus, J., Gorton, L., Varga, G.M. (1996). Peroxidase-modified electrodes: Fundamentals and application, *Anal Chim Acta., 330*, 123-138.

- Storhoff, J.J., Elghanian, R., Mucic, R.C., Mirkin, C.A., Letsinger, R.L. (1998). One-Pot Colorimetric Differentiation of Polynucleotides with Single Base Imperfections Using Gold Nanoparticle Probes, *J.Am. Chem. Soc., 120,* 1959-1964.

- Tang, D.P., Yuan, R., Chai, Y.Q., Zhong, X., Liu, Y., Dai, J.Y., Zhang, L.Y. (2004). Novel potentiometric immunosensor for hepatitis B surface antigen using a gold nanoparticle-based biomolecular immobilization method, *Anal Biochem.,* 333, 345-350.

- Tang, D., Yuan, D., Chai, Y., Dai, J., Zhong, X., Liu, Y.(2004). A novel immunosensor based on immobilization of hepatitis B surface antibody on platinum electrode modified colloidal gold and polyvinyl butyral as matrices *via* electrochemical impedance spectroscopy, *Bioelectrochem.,* 65,15–22.

- Tkachenko, A.G., Xie, H., Coleman, D., Glomm, W., Ryan, J., Anderson, M.F., Franzen, S.,Feldheim, D.L.(2003). Multifunctional

Gold Nanoparticle−Peptide Complexes for Nuclear Targeting, *J. Am. Chem. Soc.*, *125*, 4700-4701.

- Wang, M., Wang, L., Yuan, H., Ji, H., Sun, C., Ma, L., Bai, Y., Li, T., Li J. (2004). 4-Aminothiophenol Self-Assembled Monolayer for the Development of a DNA Biosensor Aimng the Detection of Cylindrospermopsin Producing Cyanobacteria, *Electroanalysis,* 16, 757-764.

- Wang, M., Wang, L., Yuan, H., Ji, H., Sun, C., Ma, L., Bai, Y., Li, T., Li J. (2004). Application of impedance spectroscopy for monitoring colloid Au-enhanced antibody immobilization and antibody–antigen reactions, *Biosens and bioelectron.,* 19, 575-582.

- Wu, Z.S., Li, J.S., Luo, M.H., Shen, G.L., Yu, R.Q. (2005). A novel capacitive immunosensor based on gold colloid monolayers associated with a sol–gel matrix, *Anal Chim Acta.*,528, 235–242.

Summary

Summary

I. Synthesis of gold nanoparticles

- We have demonstrated the synthesis and capping of gold nanoparticles using two different capping agents, glutathione and lipoic acid, the capping of gold nanoparticles, which can be used for further modifications.
- The UV-VIS spectroscopy studies showed that after the capping of gold nanoparticles, there was a shift in the wavelength from 520nm (specific plasmon resonance for gold nanoparticles) towards longer wavelength for both the glutathione and lipoic acid capped nanoparticles.
- From TEM analysis, we observed that the nanoparticles were evenly shaped with no sign of aggregation.
- The average size of the nanoparticles was around ~20nm which agrees well with the theoretical calculation using UV-VIS spectroscopy.

II. Direct electrochemistry of horseradish peroxidase-gold nanoparticles conjugate

- The cyclic voltammetry measurement showed good electrochemical response for both HRP coupled to glutathione and lipoic acid capped Au-NP. The peak potential was at E_{pc} =

0.110 V; E_{pa} = 0.182 V and E_{pc} = 0.011 V; E_{pa} = 0.089 V for glutathione and lipoic acid capped gold colloid.

- Both the glutathione and lipoic acid capped Au-NP modified electrodes showed a good electrochemical response.
- The optimal activity of HRP labeled AuNPs was between the range pH 7.2-8.0.
- This study shows that the approach of covalent linking of the enzyme to the nanoparticles needs less time as it forms a more stable attachment (no leaching). Coupled enzyme has full biochemical activity with a spacer arm, which gives a possibility of higher efficiency of electron transport.
- We propose that the HRP electrode can be successfully used as an electrochemical tool instead of a colorimetric assay, as this mode of operation is faster, more accurate and less prone to noise.
- The protocol outlined in this experiment can be used for any common enzyme with very little modifications and therefore offers the possibility of developing arrays of sensors using this covalent coupling technique.

III. <u>Gold nanoparticles based sandwich electrochemical immunosensor</u>

- This study shows the direct linking of antibody to AuNPs using a spacer arm. It not only provides the right orientation of the

antibody to bind with the antigen but also the AuNPs used has good conducting capabilities to pass the electron to the electrode for the detection.

- This electrode provides a novel means for the antibody immobilization and antibody-antigen interaction studies.
- The cyclic voltammetry measurements were done using TMB that had shown a couple of clear and well defined peaks and the detection limit was found to be 2 ng/ml or 10 pg/5µl of the sample.
- The impedance measurements showed the formation of the antibody-antigen interaction.
- We suggest that the sensitivity of the sensors is good but can be increased using flow injection system.
- We propose that this kind of approach is simple, faster and cost effective and can be used for developing an immunosensor.

Gold nanoparticles based biosensors shows clearly the potential and advantageous features of the approach to construct a biosensor exhibiting good performances. The unique properties of gold nanoparticles concerning the immobilization of biomolecules retaining their biological activity and as efficient conducting interfaces with electrocatalytic ability makes them a powerful tool to modify electrode materials and to construct robust and sensitive biosensors which can be applied in many fields. In our procedure we have demonstrated that the gold nanoparticles can be useful as interfaces for

the electrocatalysis of redox processes of molecules such as H_2O_2 involved in many significant biochemical reactions. We have shown that our label system consisting of antibody conjugated to gold nanoparticles was used to detect human IgG as model protein and can easily be extended to other proteins or analyte detection schemes.

Publications, Workshops, Conferences, Oral and Poster Presentations

Publications

1. Direct Electrochemistry of Horseradish Peroxidase-Gold Nanoparticles Conjugate. ***Sensors,*** 2009, 9, 881-894.
2. Gold Nanoparticles Based Sandwich Electrochemical Immunosensor.2009, communicated to ***Biosensors and Bioelectronics.***

Workshops, Conferences, Oral and Poster Presentations

1. International Society for Electrochemistry 4th Spring meeting "17-20 April, 2006" held at NUS, Singapore.
2. The 8th Workshop on Biosensors and Bioanalytical μ-Techniques in Environmental and Clinical Analysis, "October 3-6, 2007" held at BITS-Pilani Goa Campus, India.
3. The 12th International Symposium on Electroanalytical Chemistry (12th ISEC), "12-15 August, 2009", Changchun, China